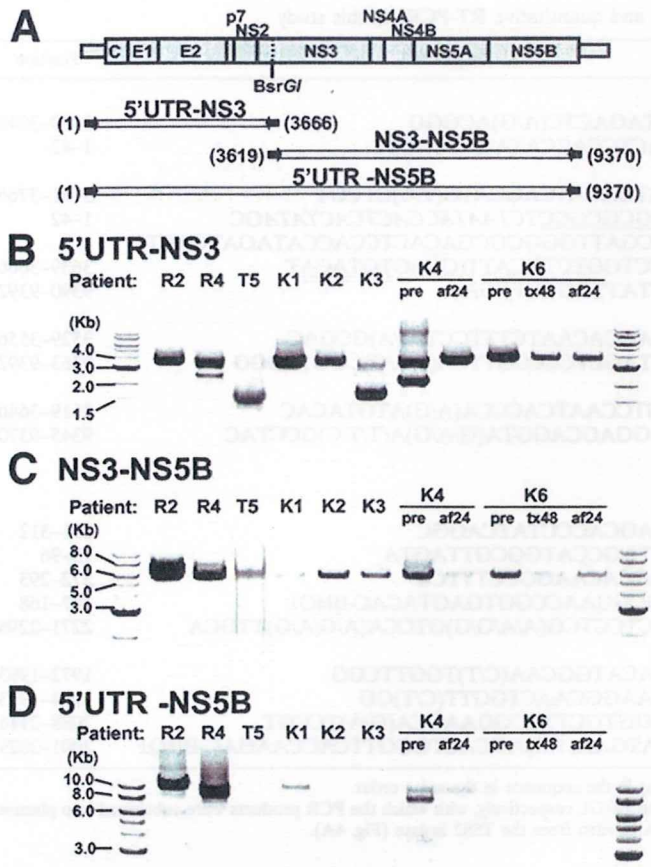

FIG. 1. Representative results of long-distance RT-PCRs for serum HCV. (A) The three sets of long-distance RT-PCR used: 5′ UTR-NS3 (5′ UTR to the 5′ part of the NS3 region), NS3-NS5B (the remaining part of the NS3 region to the end of NS5B), and 5′ UTR-NS5B (5′ UTR to the end of the NS5B region). The nucleotide positions of the 5′ and 3′ ends of each amplicon are indicated in parentheses. PCR products were electrophoresed and stained with ethidium bromide. Results of the representative 11 specimens (eight patients) are shown for 5′ UTR-NS3 (B), NS3-NS5B (C), and 5′ UTR-NS5B (D). Serum specimens were collected from patients K4 and K6 before interferon treatment (pre), at the end of the full 48-week treatment period (tx48), and 24 weeks after the full treatment period (af24). DNA molecular size markers are at both sides of panels B to D.

NS5B region, while the amplicon of the predicted size (ca. 5.6 kb) was detected in all of the specimens, albeit with various efficiencies (Fig. 1C). The 5′ UTR-NS5B region, which covers almost the whole genome, was then amplified, and an amplicon of the predicted size (9.4 kb) was detected in 10 specimens from nine patients (5 specimens in Fig. 1D). Of the successfully amplified specimens, two (R4 and K4-pre) also contained a shorter amplicon, in accordance with the results of the 5′ UTR-NS3 PCR. The NS3-NS5B region is essential for autonomous replication of HCV as an RNA replicon in vitro (5–7). It has been shown that NS5A is the only nonstructural protein that can *trans* complement HCV replication (13). They used a nonadaptive mutation of NS5A as a replication-incompetent NS5A protein instead of a deletion mutant protein. Thus, we speculate that deletion of the NS3-NS5B region cannot be complemented in *trans*. Intriguingly, the shorter amplicon was not detected after full-term interferon treatment in patient K4 (K4-af24), although it was detected prior to treatment (K4-pre) (Fig. 1B and D). The possible reasons for this are that (i) the defective genome disappeared naturally, (ii) packaging of the defective genome by the helper virus was impeded by an unknown mechanism of interferon, or (iii) replication of the defective genome is preferentially inhibited by the interferon pathway. Further studies are needed to reveal the effect of a defective HCV genome on the pathogenesis and treatment of HCV.

A total of 38 isolates with defective HCV genomes were molecularly cloned into plasmid vector pASGT (unpublished data) from the shorter amplicons of the 5′ UTR-NS3 PCR from four serum specimens (R4, T5, K3, and K4-pre in Fig. 1B) at the AscI and BsrGI restriction sites. The nucleotide sequences were determined with an autosequencer (3730 DNA analyzer; Applied Biosystems, Foster City, CA). Sequence analyses revealed that the structural region was widely deleted in all of the defective isolates and that the deletion ranges were quite diverse among the isolates (extending up to the NS2 region) (Fig. 2A). In contrast, the 5′ UTR and core regions were constantly preserved, suggesting that these regions, as well as the NS3-NS5B region, are indispensable for the production of HCV with a defective genome. Intriguingly, defective genomes with different deletion patterns coexisted in single specimens from two patients (three patterns in patient K3 and four patterns in patient K4-pre). Moreover, two deletions in a single genome were observed in five isolates from patient R4 (isolate R4S-5). As many as three deletions in a single genome were observed in the isolate from patient K3 (e.g., isolate K3S-15), in which two small deletions resulted in two tiny residual fragments. Such diversity in deletion ranges indicates flexibility of the remaining structural region for the replication of defective HCV genomes. Nevertheless, all of the deletions identified in the 38 isolates were in frame (Fig. 2B), implying that these defective HCV genomes have the potential for translation from the core to the authentic end of NS5B without a frameshift.

To determine the ratio of defective to full genomes, we performed quantitative PCRs targeting a relatively conserved E2 sequence, which is commonly deleted in the defective genomes, with primers listed in Table 1. Calculation of the 5′ UTR/E2 ratio, which must theoretically be 1 without the existence of the defective genome, showed higher values (1.7 to 2.45) in specimens containing the defective genomes (R4, K3, and K4pre in Table 2), indicating that the defective genome level in serum is 0.7 to 1.45 times the full genome level. However, to clarify the impact of defective genomes on pathogenesis and their effect on the treatment of HCV, accumulation of more data is needed.

The nucleotide sequence comparison of 38 defective HCV isolates showed sequence diversity. Such diversity was observed even among isolates obtained from the same specimen. Perhaps such diversity is a result of self-replication and the subsequent evolution of the defective HCV genome. To explore this possibility, phylogenetic analyses were performed on the nucleotide sequence data from patient K4. Sequences at the 5′ and 3′ maximum overlapping regions located outside the deletions were separately compared (Fig. 2A), and phylogenetic trees were created by the neighbor-joining method with GENETYX software (Genetyx Inc., Tokyo, Japan). As a re-

TABLE 1. Primers used for long-distance and quantitative RT-PCRs in this study

Test and region(s)	Direction	Primer(s)[a]	Sequence[b]	Position[c]
Long-distance PCR				
5′ UTR-NS3	RT	606R/712R	GTTTCCATAGACTC(A/G)ACGGG	3930–3949
5′ UTR-NS3, 5′ UTR-NS5B	1st forward	420	GGCGACACTCCACCATAGATCACTC	1–42
5′ UTR-NS3	1st reverse	605R/713R	ACCGGAATGACATCAGCATG(T/C)CTCGT	3741–3766
5′ UTR-NS3, 5′ UTR-NS5B	2nd forward	AscT7-420	ATCGTAGGCGCGCCTCTAATACGACTCACTATAGC CAGCCCCCGATTGGGGGCGACACTCCACCATAGATCACTC	1–42
5′ UTR-NS3	2nd reverse	604R/714R	CGAGGTCCTGGTCTACATT(G/A)GTGTACAT	3639–3666
NS3-NS5B, 5′ UTR-NS5B	RT	386R	AATGGCCTATTGGCCTGGAG	9390–9392
NS3-NS5B	1st forward	602/723	CCACCGCAACACAATCTTTCCT(G/A)GCGAC	3529–3556
NS3-NS5B, 5′ UTR-NS5B	1st reverse	719R/720R/721R	GAGTGTTTAGCTCCCCGTTCA(T/C/G)CGGTTGGG	9363–9392
NS3-NS5B	2nd forward	603/724	CAAAGGGTCCAATCACCCA(A/G)ATGTACAC	3619–3646
NS3-NS5B, 5′ UTR-NS5B	2nd reverse	607R/654R/722R	CGGTTGGGGAGCAGGTA(G/A/G)A(T/T/C)GCCTAC	9345–9370
Quantitative PCR				
5′ UTR	RT	738RH	ACTCGCAAGCACCCTATCAGGC	291–312
5′ UTR	Forward	736	AAGCGTCTAGCCATGGCGTTAGTA	73–96
5′ UTR	Reverse	737R	GGCAGTACCACAAGGCCTTTCG	272–293
5′ UTR	Probe	733FB	FAM-TCTGCGGAACCGGTGAGTACAC-BHQ1	147–168
E2	RT	743RH/744RH/753RH/753RH	CAACGCTCTCCTCG(A/A/G/G)GTCCA(A/G/A/G)TTGCA	2271–2296
E2	Forward[d]	751/752	GGCCTCCACATGGCAA(C/T)TGGTTCGG	1972–1993
E2	Forward[d]	739/740	CCGCCGCAAGGCAACTGGTT(C/T)GG	1974–1993
E2	Reverse	741R/742R	GCCTCGGGGTGCTTCCGGAAGCA(G/A)TCCGT	2088–2116
E2	Probe	734FB/735FB	FAM-TGGATGAA(T/C)AGCACTGGGTTCACCAAGAC-BHQ1	2001–2029

[a] Primers separated by slashes harbor a nucleotide substitution(s) (in parentheses) in the sequence in the same order.
[b] An underline and a double underline indicate recognition sequences for AscI and BsrGI, respectively, with which the PCR products were subcloned into plasmid vector pASGT5. Italics denote the T7 promoter, which was used to synthesize RNA in vitro from the T5S2 isolate (Fig. 4A).
[c] Nucleotide positions correspond to the HCV-JS sequence (12).
[d] Forward primers for E2 were mixed in the reaction mixture.

sult, isolates with the same deletion pattern formed genetic clusters that were distinct from each other, as well as from those of nondefective HCV isolates (Fig. 3A and B). Similar results were obtained for the other patients with defective HCV genomes (data not shown). These results suggest that a defective HCV genome is capable of replication to accumulate mutations and to evolve independently of the nondefective HCV genome.

TABLE 2. Quantitative PCRs for the 5′ UTR and E2 regions of HCV[a]

Region for quantification	No. of copies/ml		5′ UTR/E2 ratio
	5′ UTR	E2	
R2	2.0×10^6	1.7×10^6	1.17
R4	5.3×10^6	2.2×10^6	2.44
T5	ND[b]	ND[b]	
K1	8.3×10^5	8.4×10^5	0.99
K2	3.6×10^5	3.5×10^5	1.01
K3	8.6×10^5	5.1×10^5	1.7
K4pre	8.1×10^5	3.3×10^5	2.45
K4af24	4.5×10^5	4.4×10^5	1.01

[a] For quantification of the 5′ UTR and E2 regions, the TaqMan Fast PCR Universal mixture and the 7500 Fast Real-Time PCR system (Applied Biosystems) were used in a two-step method with the primers and probes shown in Table 1 according to the manufacturer's protocol. The copy number of HCV was determined by the standard-curve method with serial dilutions of the synthesized full-length HCV RNA.
[b] ND, not determined due to sample shortage.

Next, the ability of the defective HCV genome to be encapsidated and released from cells as HCV_{CCD} was examined. A genotype 1b replicon RNA lacking the structural region was synthesized by using defective isolate T5S-2 from patient T5 (Fig. 2 and 4A) as the template in an in vitro transcription system (MEGAscript T7 kit; Ambion, Inc., Austin, TX) under the control of the T7 promoter. Also, capped mRNA encoding the genotype 1b structural proteins from the same patient (designated C-NS2 in Fig. 4A) was synthesized in vitro with the mMessage mMachine T7 kit (Ambion). Both synthesized RNAs were cotransfected into Huh7.5 hepatoma cells. However, HCV_{CCD} was not obtained, presumably because of low replication or virus productivity of genotype 1b HCV per se. In fact, we transfected the defective RNA alone and observed the replication and protein expression of HCV, but with low efficiency (data not shown). Thus, to augment virus productivity, a JFH1-based chimeric HCV genome (genotype 1b/2a) and its deletion mutant were generated to mimic isolate T5S-2 (designated TNS2J1 and TNS2J1ΔS, respectively, Fig. 4A). JFH1 is genotype 2a HCV isolate that can produce high levels of infectious virus (14). To verify the virus productivity of TNS2J1, Huh7.5 cells (10-cm plate) were transfected with 10 μg of in vitro-synthesized RNA from TNS2J1 or JFH1 by lipofection with TransMessenger transfection reagent (Qiagen, Valencia, CA) according to the manufacturer's protocol. Two days later, the culture medium was concentrated 10-fold and inoculated into naïve Huh7.5 cells (four-well chamber

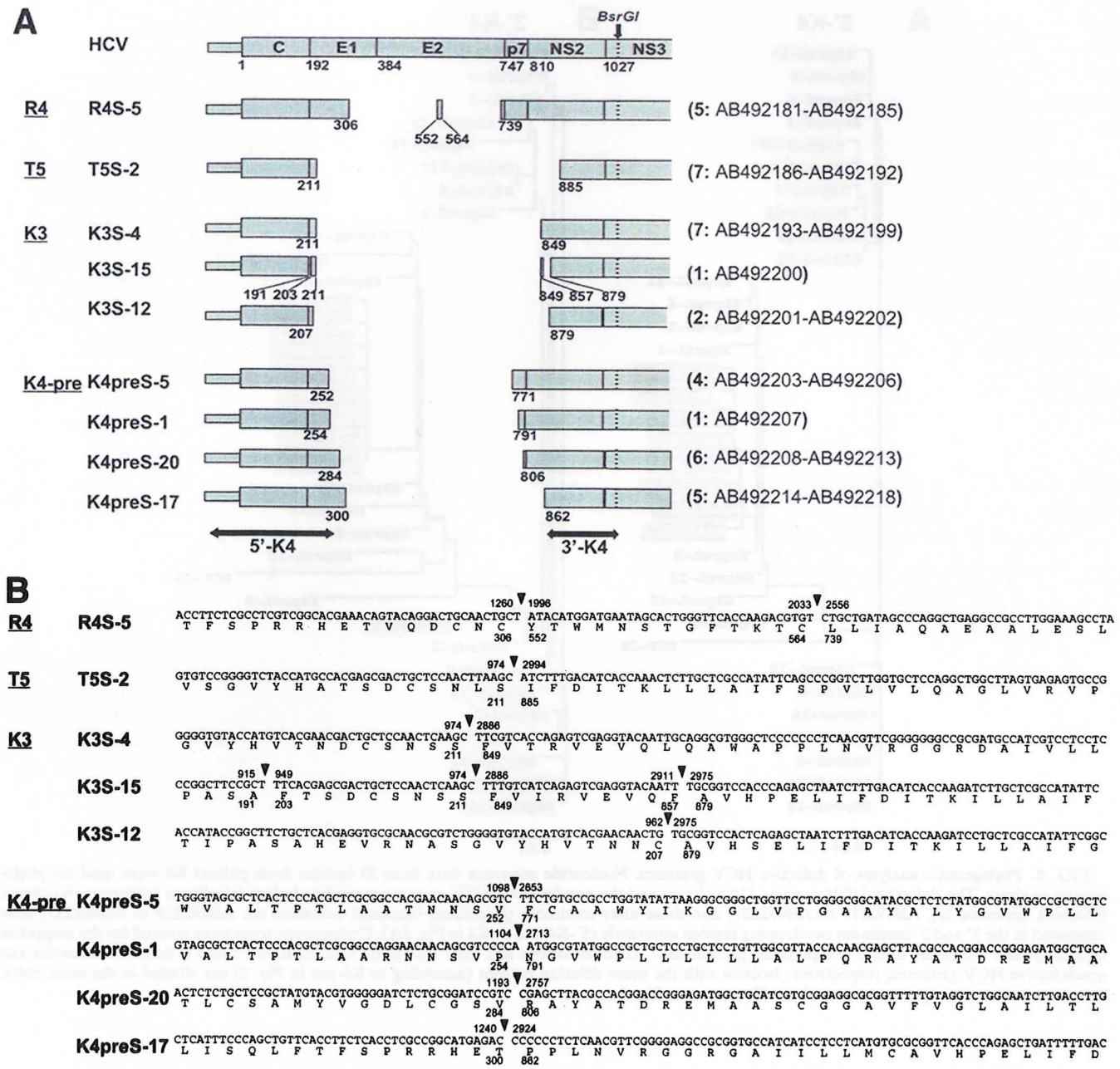

FIG. 2. Sequence analysis of the defective HCV genomes. A total of 38 isolates were molecularly cloned into a plasmid vector and sequenced. Data from representative isolates are presented. Nucleotide positions and deduced amino acid positions correspond to those of genotype 1b strain HCV-JS (12). (A) Defects located in the structural region were compared. The remaining regions are illustrated as shaded boxes. Below the boxes are numbers indicating amino acid positions at the end of each remaining region. At the top of the panel is the HCV genome with the amino acid position at the N terminus of each HCV protein below. The BsrGI restriction site that was used to clone the PCR products is shown as a dotted line. Each value in parentheses at the right is the number of isolates showing the same deletion pattern, followed by the GenBank accession number(s). The two-headed arrows indicate the 5′ and 3′ maximum overlapping regions among the defective HCV isolates in the K4-pre specimen that are compared in the following phylogenetic analyses (5′-K4 and 3′-K4; see Fig. 3). (B) Deletion breakpoints and their adjacent nucleotides and deduced amino acid sequences are indicated. Solid triangles denote breakpoints, and numbers indicate the nucleotide positions (above) and amino acid positions (below) at the junctions.

slide). Cells inoculated with the culture medium from TNS2J1 RNA-transfected cells markedly expressed HCV protein, as shown by immunofluorescent staining (Fig. 4B). The percentage of HCV-positive cells in chimera-infected cells, 40% (565/1,240), was greater than that of JFH1, 3% (37/1,210), demonstrating that the chimeric genome TNS2J1 can produce infectious HCV more robustly than JFH1 can ($P < 0.0001$).

Taking advantage of this chimeric genome, we conducted *trans* complementation experiments. To mimic the T5S-2 iso-

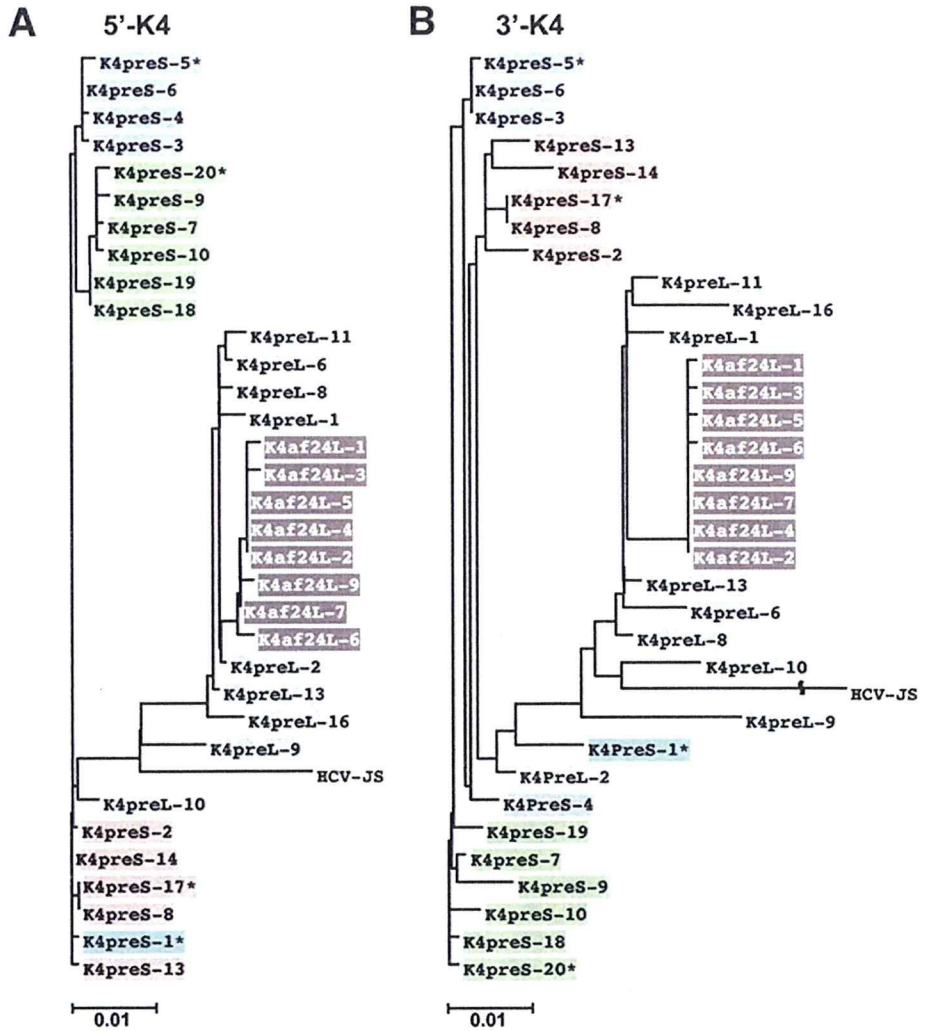

FIG. 3. Phylogenetic analyses of defective HCV genomes. Nucleotide sequence data from 33 isolates from patient K4 were used for phylogenetic analyses. The defective HCV genome (16 isolates) and the nondefective HCV genome coexisting before interferon treatment (9 isolates; GenBank accession no. AB492219 to AB492227) and those after treatment (8 isolates; GenBank accession no. AB492228 to AB492235) were compared in the 5′ and 3′ maximum overlapping regions separately (5′-K4 and 3′-K4 in Fig. 2A). Phylogenetic trees were created for the respective regions (A and B). In the isolate designations, pre and af24 stand for before and after interferon treatment and S and L stand for defective and nondefective HCV genomes, respectively. Isolates with the same deletion pattern (according to K4-pre in Fig. 2) are shaded in the same color. Asterisks denote the representative isolates illustrated in Fig. 2.

late, the region corresponding to the defect found in T5S-2 was identically deleted from the TNS2J1 genome (designated TN2J1ΔS, Fig. 4A). Ten micrograms of synthesized RNA of TN2J1ΔS was cotransfected into Huh7.5 cells (10-cm plate) together with 10 μg of synthesized capped mRNA encoding the structural region, including part of the nonstructural region of TNS2J1, designated C-NS2 or C-NS3P (Fig. 4A). Two days later, the culture medium was concentrated and inoculated into naïve Huh7.5 cells as previously described. HCV protein was expressed when cells were inoculated with the medium of cells cotransfected with TN2J1ΔS RNA and C-NS2 or C-NS3P mRNA, whereas no expression was observed in the case of TN2J1ΔS RNA alone (Fig. 4C). To stably provide the structural proteins in *trans*, packaging cell lines were established by retroviral transduction (2) of Huh7.5 cells with genes encoding the C-NS2 or C-NS3P region (Fig. 4A). These packaging cell lines were transfected with TN2J1ΔS RNA, and HCV protein was expressed in cells inoculated with the culture medium from the RNA-transfected packaging cells (Fig. 4D). Notably, the construct C-NS2 helped to produce HCV_{CCD} more efficiently than C-NS3P did (Fig. 4C). We observed less expression of the structural proteins with the C-NS3 construct than with the C-NS2 construct in a transient expression experiment (data not shown). One possible reason for this is that the C-NS3 construct needs one additional process, i.e., cleavage between NS2 and NS3, to produce NS2 and may affect the other proteins. Otherwise, it is simply because of the difference in the lengths of the constructs. These results indicate that a defective HCV genome lacking the structural region can be encapsidated by *trans* complementation of the structural proteins, thus conferring infectivity in vivo. Recently, a *trans*-packaging system consisting of an HCV subgenomic replicon and a reporter gene

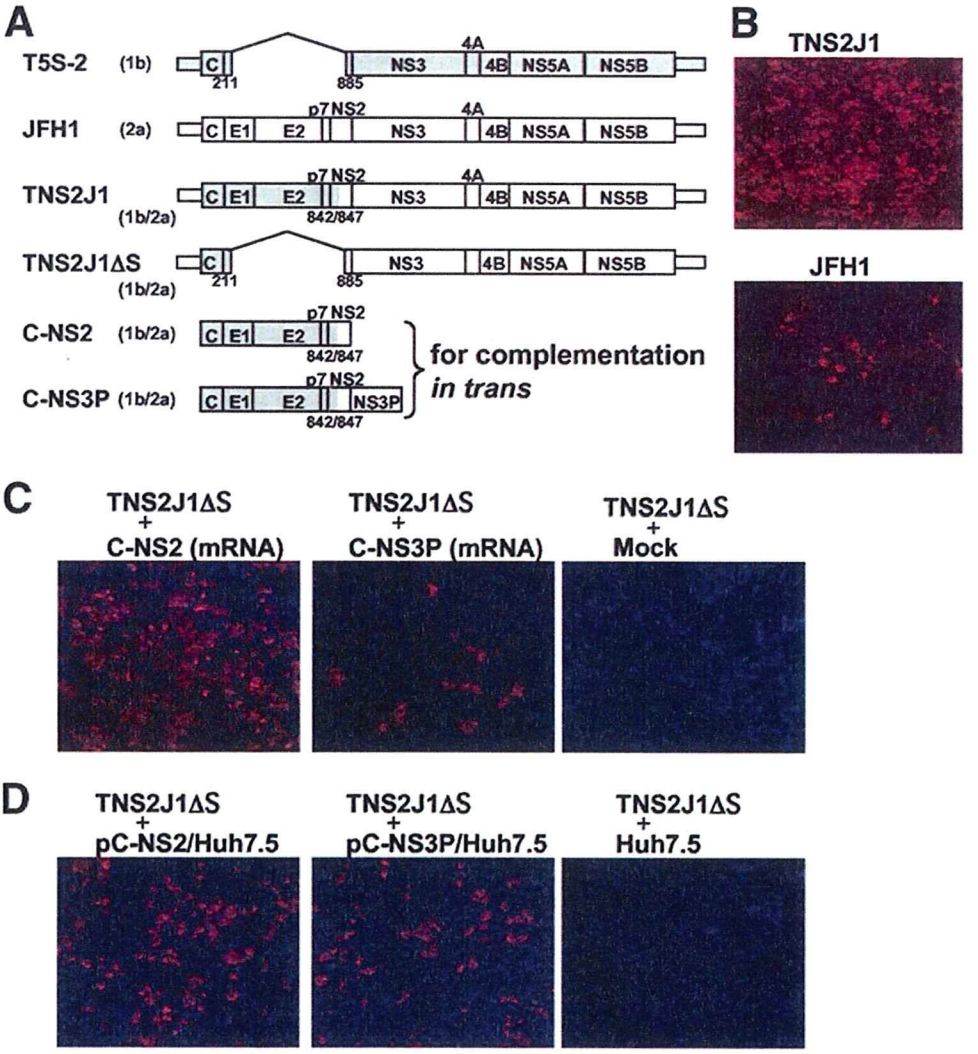

FIG. 4. In vitro infectivity of deletion mutant of chimeric HCV conferred by *trans* complementation of structural proteins. (A) Schematics of the following HCV genomic constructs: the defective HCV isolate (T5S-2), JFH1, chimeric virus of genotypes 1b and 2a (TNS2J1), and its deletion mutant (TNS2J1ΔS). C-NS2 and C-NS3 are fragments encoding the region from the core to the C terminus of the NS2 region and to the C terminus of the serine protease moiety in NS3, respectively. For the *trans* complementation experiments, the latter two constructs were inserted into pcDNA3.1 (Invitrogen) to synthesize capped mRNAs or into retroviral vector pCX4bsr (GenBank accession no. AB086384) to establish packaging cell lines stably expressing the proteins. Shaded and open boxes represent genotypes 1b (isolate from patient T5) and 2a (JFH1), respectively. The numbers below the boxes are amino acid positions at deletion breakpoints or at PCR-based recombination junctions. Naïve Huh7.5 cells were inoculated with the culture medium from cells transfected with JFH1 or TNS2J1 RNA (B), from cells cotransfected with TNS2J1ΔS RNA together with the structural region mRNA (C-NS2 or C-NS3P) or TNS2J1ΔS RNA alone (C), and from the packaging cell line (C-NS2/Huh7.5 or C-NS3P/Huh7.5) transfected with TNS2J1ΔS RNA and parental Huh7.5 cells transfected with TNS2J1ΔS RNA (D). HCV protein was detected by human HCV serum (1:500) by the indirect immunofluorescent method with Alexa Fluor 568 goat anti-human immunoglobulin G (1:200; red; Invitrogen). Nuclei were counterstained with 4′,6′-diamidino-2-phenylindole (DAPI; blue).

was also reported in which an intragenotypic chimera (2a/2a) was used as the most efficient packaging construct (11). Our packaging system used an efficient intergenotypic chimera (1b/2a) to encapsidate a genome mimicking a naturally occurring deletion (1b). Thus, although its efficiency may be different, our system could be a useful tool for the study of HCV_{CCD} of chimeric genome 1b/2a or genotype 1b.

Taken together, genetic analyses of the defective HCV genome showed the potential of its translation and self-replication. These defective genomes can be encapsidated into infectious virus-like particles by *trans* complementation of the structural proteins in vitro. The 5′ UTR and core regions, which are preserved in defective HCV genomes, are targets for the clinical quantification of HCV. Therefore, measured values may represent additive values for defective and nondefective HCVs and the method used for HCV quantification should be reevaluated.

We thank H. Kato, R. Shiina, and H. Yamamoto for technical assistance; T. Wakita for the gift of JFH1; C. Rice for the gift of Huh7.5 cells; and T. Akagi for the gift of retroviral vector pCX4bsr.

This work was supported by a grant-in-aid for scientific research (C) from the Japan Society for the Promotion of Science (KAKENHI18590454) and a grant-in-aid for research on hepatitis from the Ministry of Health, Labor, and Welfare.

REFERENCES

1. **Brinton, M. A.** 1983. Analysis of extracellular West Nile virus particles produced by cell cultures from genetically resistant and susceptible mice indicates enhanced amplification of defective interfering particles by resistant cultures. J. Virol. **46**:860–870.
2. **Chen, C. J., K. Sugiyama, H. Kubo, C. Huang, and S. Makino.** 2004. Murine coronavirus nonstructural protein p28 arrests cell cycle in G_0/G_1 phase. J. Virol. **78**:10410–10419.
3. **Huang, A. S., and D. Baltimore.** 1970. Defective viral particles and viral disease processes. Nature **226**:325–327.
4. **Iwai, A., H. Marusawa, Y. Takada, H. Egawa, K. Ikeda, M. Nabeshima, S. Uemoto, and T. Chiba.** 2006. Identification of novel defective HCV clones in liver transplant recipients with recurrent HCV infection. J. Viral Hepat. **13**:523–531.
5. **Kato, N., K. Sugiyama, K. Namba, H. Dansako, T. Nakamura, M. Takami, K. Naka, A. Nozaki, and K. Shimotohno.** 2003. Establishment of a hepatitis C virus subgenomic replicon derived from human hepatocytes infected in vitro. Biochem. Biophys. Res. Commun. **306**:756–766.
6. **Kishine, H., K. Sugiyama, M. Hijikata, N. Kato, H. Takahashi, T. Noshi, Y. Nio, M. Hosaka, Y. Miyanari, and K. Shimotohno.** 2002. Subgenomic replicon derived from a cell line infected with the hepatitis C virus. Biochem. Biophys. Res. Commun. **293**:993–999.
7. **Lohmann, V., F. Körner, J. Koch, U. Herian, L. Theilmann, and R. Bartenschlager.** 1999. Replication of subgenomic hepatitis C virus RNAs in a hepatoma cell line. Science **285**:110–113.
8. **Noppornpanth, S., S. L. Smits, T. X. Lien, Y. Poovorawan, A. D. Osterhaus, and B. L. Haagmans.** 2007. Characterization of hepatitis C virus deletion mutants circulating in chronically infected patients. J. Virol. **81**:12496–12503.
9. **Poidinger, M., R. J. Coelen, and J. S. Mackenzie.** 1991. Persistent infection of Vero cells by the flavivirus Murray Valley encephalitis virus. J. Gen. Virol. **72**(Pt. 3):573–578.
10. **Shimotohno, K.** 1995. Hepatitis C virus as a causative agent of hepatocellular carcinoma. Intervirology **38**:162–169.
11. **Steinmann, E., C. Brohm, S. Kallis, R. Bartenschlager, and T. Pietschmann.** 2008. Efficient *trans*-encapsidation of hepatitis C virus RNAs into infectious virus-like particles. J. Virol. **82**:7034–7046.
12. **Sugiyama, K., N. Kato, T. Mizutani, M. Ikeda, T. Tanaka, and K. Shimotohno.** 1997. Genetic analysis of the hepatitis C virus (HCV) genome from HCV-infected human T cells. J. Gen. Virol. **78**(Pt. 2):329–336.
13. **Tong, X., and B. A. Malcolm.** 2006. Trans-complementation of HCV replication by non-structural protein 5A. Virus Res. **115**:122–130.
14. **Wakita, T., T. Pietschmann, T. Kato, T. Date, M. Miyamoto, Z. Zhao, K. Murthy, A. Habermann, H. G. Krausslich, M. Mizokami, R. Bartenschlager, and T. J. Liang.** 2005. Production of infectious hepatitis C virus in tissue culture from a cloned viral genome. Nat. Med. **11**:791–796.
15. **Yagi, S., K. Mori, E. Tanaka, A. Matsumoto, F. Sunaga, K. Kiyosawa, and K. Yamaguchi.** 2005. Identification of novel HCV subgenome replicating persistently in chronic active hepatitis C patients. J. Med. Virol. **77**:399–413.
16. **Yoon, S. W., S. Y. Lee, S. Y. Won, S. H. Park, S. Y. Park, and Y. S. Jeong.** 2006. Characterization of homologous defective interfering RNA during persistent infection of Vero cells with Japanese encephalitis virus. Mol. Cells **21**:112–120.

Cancer Science
The official journal of the Japanese Cancer Association JCA

Identification of cellular and viral factors related to anti-hepatitis C virus activity of cyclophilin inhibitor

Kaku Goto,[1] Koichi Watashi,[1,2] Daisuke Inoue,[1] Makoto Hijikata[1] and Kunitada Shimotohno[1,3,4]

[1]Laboratory of Human Tumor Viruses, Department of Viral Oncology, Institute for Virus Research, Kyoto University, Kyoto, Japan; [2]Molecular Virology Section, Laboratory of Molecular Microbiology, National Institute of Allergy and Infectious Diseases, National Institutes of Health, Bethesda, Maryland, USA; [3]Research Center, Chiba Institute of Technology, Chiba, Japan

(Received April 25, 2009/Revised June 8, 2009/Accepted June 16, 2009/Online publication July 30, 2009)

We have so far reported that an immunosuppressant cyclosporin A (CsA), a well-known cyclophilin (CyP) inhibitor (CPI), strongly suppressed hepatitis C virus (HCV) replication in cell culture, and that CyPB was a cellular cofactor for viral replication. To further investigate antiviral mechanisms of CPI, we here developed cells carrying CsA-resistant HCV replicons, by culturing the HCV subgenomic replicon cells for 4 weeks in the presence of CsA with G418. Transfection of total RNA from the isolated CsA-resistant cells to naïve Huh7 cells conferred CsA resistance, suggesting that the replicon RNA itself was responsible for the resistant phenotype. Of the identified amino acid mutations, D320E in NS5A conferred the CsA resistance. The replicon carrying the D320E mutation was sensitive to interferon-α, but was resistant to CsA and other CPIs including NIM811 and sanglifehrin A. Knockdown of individual CyP subtypes revealed CyP40, in addition to CyPA and CyPB, contributed to viral replication, and CsA-resistant replicons acquired independence from CyPA for efficient replication. These data provide important evidence on the mechanisms underlying the regulation of HCV replication by CyP and for designing novel and specific anti-HCV strategies with CPIs. (*Cancer Sci* 2009; 100: 1943–1950)

Hepatitis C virus (HCV) is a leading cause of chronic hepatitis, liver cirrhosis, and hepatocellular carcinoma (HCC), and affects an estimated 170 million people worldwide.[1] The current standard therapy for patients infected with HCV is the combination treatment with pegylated interferon and ribavirin.[2,3] However, approximately half of individuals infected with HCV are unable to reach sustained virological response following such treatment. In addition, several side effects have been reported, which hinder continued treatment and impair the regimen efficacy. Thus, the development of novel anti-HCV strategies is essential for the treatment of infected individuals.

We have previously reported that a well-known immunosuppressant cyclosporin A (CsA) strongly suppressed the replication of HCV *in vitro*, in a manner independent of the interferon (IFN) signal transduction pathway.[4] Cyclophilin B (CyPB), a cellular target of CsA, was subsequently revealed to facilitate viral replication via the regulation of the RNA binding ability of NS5B.[5] Thus CyP, in addition to viral proteins including NS3 protease and NS5B polymerase, can also prove useful as a molecular target for antiviral strategies. Indeed, the non-immunosuppressive CsA analogs NIM811, DEBIO-025, and SCY635 have been observed to exert strong inhibitory effects on HCV replication, and these compounds are now in clinical trial.[6–8] Thus, it is crucial to deepen understanding of the anti-HCV actions of cyclophilin inhibitor (CPI) in order to maximize the efficacy of the agent. CPIs also need to face challenges such as side effects and drug resistance, which was observed as barrier to successful treatment in cases of human immunodeficiency virus (HIV),[9–12] and further clarification of the mechanism of CPI's anti-HCV activities is vital for the development of stronger and more specific therapeutic drug types. For this purpose, we here established and characterized the resistant replicon to CPIs using the subgenomic replicon system. We found that D320E, a mutation in NS5A, conferred resistance to CsA on the replicon, while additional mutations in NS3, Q86R and I252T seen in our CsA-resistant clone affected the replication fitness positively and negatively, respectively. The CsA-resistant replicons with the D320E mutation showed cross-resistance to other CPIs, NIM811 and sanglifehrin A (SFA), which were thus verified to suppress HCV replication through targeting CyP, and those resistant replicons were inhibited by treatment with IFNα as effectively as the wild type. Knockdown of individual CyP subtypes in the wild-type and CsA-resistant replicon cells revealed that CyP40, besides CyPA and CyPB, played important roles in HCV replication, and CyPA was related to the CsA-resistance. These results are important for elucidating additional mechanisms of the regulation of HCV replication by CyP and also for designing novel and specific anti-HCV strategies with CPI.

Materials and Methods

Compounds. CsA and IFNα were purchased from Merck Biosciences (San Diego, CA, USA) and Otsuka Pharmaceutical (Tokyo, Japan), respectively. NIM811 and SFA were generously provided by Novartis (Basel, Switzerland).

Cell culture. MH14 cells were cultured in Dulbecco's modified Eagle's medium (Invitrogen, Carlsbad, CA, USA) with 10% fetal bovine serum, nonessential amino acids (Invitrogen), and L-glutamine (Invitrogen) in the presence of 700 μg/mL G418 (Invitrogen).

Establishment of cell clones. We established each cell clone along with the outline shown in Figure 1. CsR#4, CsR#10, and CsR#11 cells were established through the selection of MH14#12 cell colonies in the presence of 1000 μg/mL G418 and 2 μg/mL CsA. CsR#11-2 and CsR#11-3 cells were established from Huh7 cells transfected with total RNAs extracted from CsR#11 cells in the presence of 700 μg/mL G418. Q86R, D320E, Q86R/D320E, and Q86R/I252T/D320E cells were produced by 700 μg/mL G418 selection of Huh7 cells transfected with 5 μg RNA transcribed from pMH14 carrying the individual mutations Q86R in NS3 and D320E in NS5A, double mutations Q86R in NS3 and D320E in NS5A, and triple mutations Q86R in NS3, I252T in NS3, and D320E in NS5A, respectively.

Colony formation assay. MH14 cells were treated with either CsA or NIM811 in the presence of 700 μg/mL G418 for 4 weeks, followed by fixation and staining with crystal violet.

[4]To whom correspondence should be addressed.
E-mail: kunitada.shimotono@it-chiba.ac.jp

doi: 10.1111/j.1349-7006.2009.01263.x

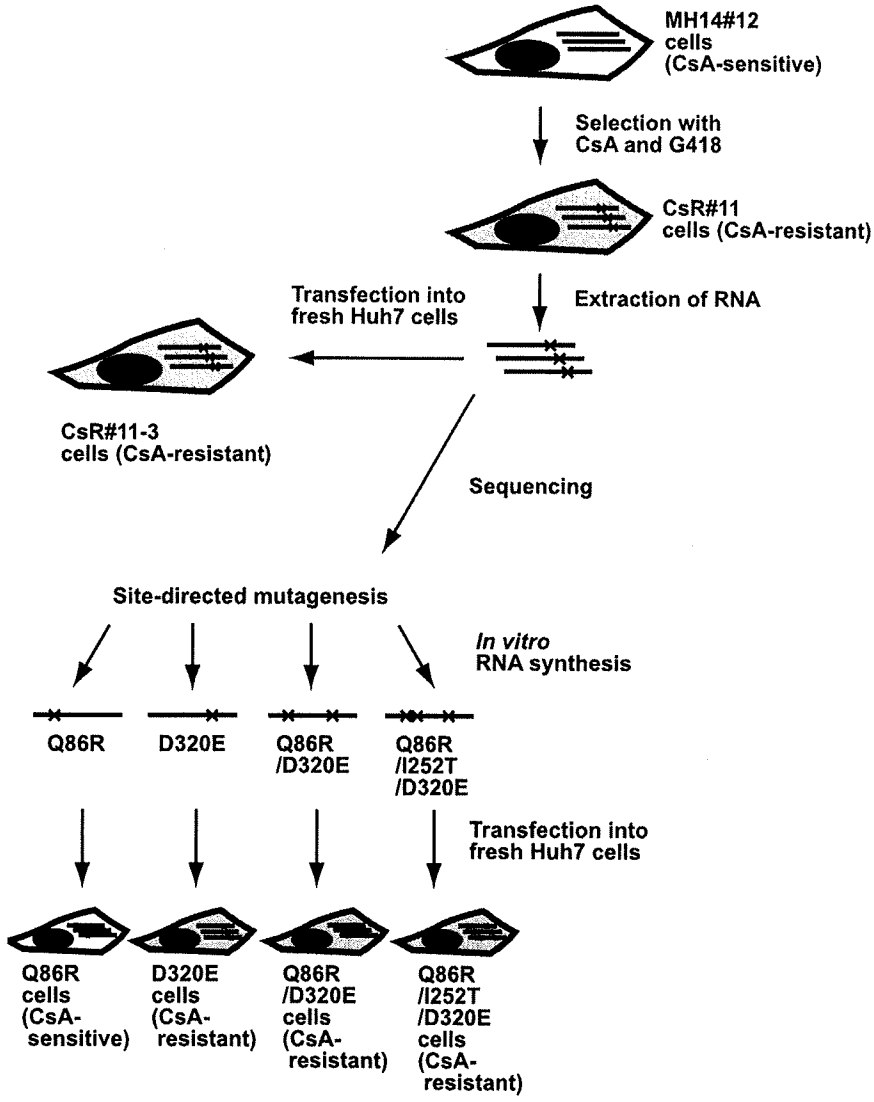

Fig. 1. Schematic diagram outlining the production of individual cell clones carrying hepatitis C virus (HCV) subgenomic replicons. MH14#12 cells, carrying wild-type HCV subgenomic repicon, were treated with 2 μg/mL cyclosporin A (CsA) in the presence of 1000 μg/mL G418 and CsR#11 cells were selected. Total RNA was extracted from CsR#11 cells and transduced into naïve Huh7 cells to select CsR#11-3 cells, and sequencing of the replicon RNA in CsR#11 cells identified mutations, Q86R in NS3, I252T in NS3, and D320E in NS5A. Site-directed mutagenesis followed by *in vitro* RNA synthesis generated HCV replicon RNA carrying Q86R, D320E, Q86R/D320E, and Q86R/I252T/D320E mutations. Transduction of the RNA into naïve Huh7 cells resulted in the production of Q86R, D320E, Q86R/D320E, and Q86R/I252T/D320E cells. The sensitivity of each replicon clone to CsA is presented as 'CsA-resistant' or 'CsA-sensitive'.

Real-time RT-PCR analysis. The 5′-non-translated region of HCV-RNA was quantified using an ABI Prism 7500 sequence detector (Applied Biosystems, Foster City, CA, USA), as previously described.[4]

Replicon sequencing. Total RNA from replicon cells was extracted with sepasol-RNA I Super (Nacalai Tesque, Kyoto, Japan) and subjected to RT-PCR reaction using super script III (Invitrogen). The products were then amplified by dividing the whole HCV region into approximately 300 bp using appropriate primer sets, and the sequence of the entire region encoding non-structural proteins was determined.

Plasmid construction. The Q86R and I252T mutations in NS3 and the D320E mutation in NS5A were generated via site-directed mutagenesis using the following primer sets: Q86R (S) 5′-AGGACCTCGTCGGCTGGCGGGCGCC-3′ plus Q86R (AS) 5′-GGCGCCCGCCAGCCGACGAGGTCCT-3′, I252T (S) 5′-AACACCAGAACTGGGGTAAGGACCA-3′ plus I252T (AS) 5′-TGGTCCTTACCCCAGTTCTGGTGTT-3′, and D320E (S) 5′-GAGTATAATCCTCCACTGCTAGAGC-3′ plus D320E (AS) 5′-GCTCTAGCAGTGGAGGATTATACTC-3′, respectively. The PCR products carrying either Q86R in NS3, I252T in NS3, or D320E in NS5A were inserted into the NotI-MluI and MluI-XbaI sites of pMH14, respectively. The resultant plasmids were termed pMH14 (Q86R), pMH14 (I252T), and pMH14 (D320E) respectively. The double mutant carrying both Q86R and D320E mutations was produced by exchanging the MluI-XbaI region of pMH14 (Q86R) with that of pMH14 (D320E), and termed pMH14 (Q86R/D320E). The triple mutant carrying Q86R, I252T, and D320E was produced by exchanging the Not-MluI region of pMH14 (D320E) with the fragments amplified by the primer set, I252T (S) plus I252T (AS), using pMH14 (Q86R) as templates for the PCR reaction. Sequence analysis of the resultant plasmids was also undertaken for confirmation of the mutations.

***In vitro* RNA synthesis.** Wild-type and mutant RNA of pMH14 was prepared by *in vitro* transcription using the MEGAscript T7 kit (Ambion, Austin, TX, USA), as described previously.[13]

Electroporation and colony formation. 8×10^6 cells suspended in 400 μL of cytomix buffer (120 mM KCl, 0.15 mM $CaCl_2$, 10 mM K_2HPO_4, 25 mM HEPES, 2 mM EGTA, and 5 mM $MgCl_2$, together with 2 mM ATP, 5 mM reduced form of glutathione, and 1.25 % DMSO) were electroporated at 250 V, 950 μF with either 100 μg total RNA extracted from replicon cells or 5 μg RNA transcribed *in vitro* from the HCV replicon construct cDNA. Cells were then treated with 1000 μg/mL G418 for 4 weeks following electroporation.

RNAi. Validated siRNAs against CyPB were purchased from Invitrogen. SiRNA duplexes against CyPA (siCyPA161, 5′-UCUGUGAAAGCAGGAACCCUU-3′; siCyPA285, 5′-GAUG

doi: 10.1111/j.1349-7006.2009.01263.x

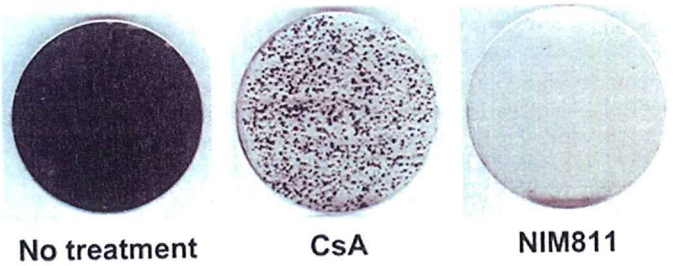

Fig. 2. Cyclophilin (CyP) inhibitor (CPI)-resistant colony emergence. MH14#12 cells were treated either without (left panel) or with 2 μg/mL CPIs, cyclosporin A (CsA) (middle panel), and NIM811 (right panel), in the presence of 700 μg/mL G418. Following 4 weeks in culture, cells were fixed and stained with crystal violet.

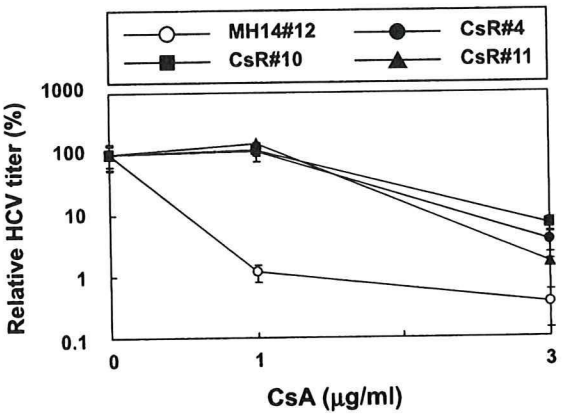

Fig. 3. Cyclosporin A (CsA) responses of the hepatitis C virus (HCV) replicon clones surviving the selection with CsA and G418. MH14#12 cells and three MH14#12-derived cell clones that survived double selection with G418 and CsA, CsR#4, CsR#10, and CsR#11, were treated with 1 and 3 μg/mL CsA for 7 days, and the HCV-RNA titers were measured by real-time RT-PCR. The data represent the percentage of HCV-RNA level in cells either untreated or treated with CsA, and the dots represent the means of three independent experiments.

CCAGGACCCGUAUGCUU-3′; siCyPA459, 5′-CUUCUUG CUGGUCUUGCCAUU-3′) were synthesized (Yahima Pure Chemicals, Osaka, Japan). SiRNAs against CyP40 were purchased from Invitrogen (siCyP40-3) and from Ambion (siCyP40-4). Pre-designed siRNAs, siCyPC, siCyPE, siCyPF, and siCyPG were obtained from Ambion. Transfection was performed using Lipofectamine RNAiMAX Transfection Reagent (Invitrogen) with 20 nM siRNAs in the absence of CsA according to the manufacturer's protocol.

Reverse transcription–polymerase chain reaction (RT-PCR) analysis. RT-PCR was performed as described previously[4] using the following primer sets: 5′-TGTTCTTCGACATTGCCGTC-3′ and 5′-CAGTCTTGGCAGTGCAGATG-3′ to detect mRNA for CyPA, 5′-TCTCCGAACGCAACATGAAG-3′ and 5′-CTGCGA TGATCACATCCTTC-3′to detect mRNA for CyPB, 5′-GGCGCA CTTGTGTTTTCTTC-3′ and 5′-TGCCATAGTGCTTCAGCTTG-3′ to detect mRNA for CyPC, 5′-TTTCGTGCACTGTGTACAGG-3′ and 5′-TTGGCTCTATCTGCTGTCTC-3′ to detect mRNA for CyP40, 5′-AGAGGAAGTGGACGACAAAG-3′ and 5′-GATGTCCATGTACACCTGAG-3′ to detect mRNA for CyPE, 5′-TGGAGCTGAAGGCAGATGTC-3′ and 5′-ACGTGACCG AACACAACATG-3′ to detect mRNA for CyPF, 5′-GAGTTGT CTCTTTCACAGAG-3′ and 5′-AACTGAGTATCCGTACCTCC-3′ to detect mRNA for CyPG, and 5′-ATGGGGAAGGTGAA GGTCGG-3′ and 5′-TGGAGGGATCTCGCTCCTGG-3′ to detect glyceraldehydes-3-phosphate dehydrogenase (GAPDH).

Results

Resistance emergence against individual CPIs. We have previously demonstrated the robust anti-HCV activities of CPIs, and it was reported that CPI significantly decreased HCV viral load in HCV-infected patients.[14,15] The problem of the drug-resistant HCV variants, hence, should be assessed *in vitro*, considering that practical efficacies of these inhibitors with long-term effectiveness are required in patients. In the first step of this study, we investigated the emergence of drug resistant replicon against CPIs. We treated MH14#12 cells, Huh7 cells carrying wild-type MH14 replicon with 2 μg/mL CsA, or the non-immunosuppressive analog NIM811 in the presence of 700 μg/mL G418 for 4 weeks. To visualize the appearance of drug-resistant clones, we stained cells after the selection. We observed colonies resistant to CsA, while we obtained few colonies under the treatment with the same concentration of NIM811 (Fig. 2).

Isolation and characterization of replicon cells resistant to CsA. To characterize the CsA-resistant HCV, we isolated the resistant clones following selection with 2 μg/mL CsA and 1000 μg/mL G418 for 4 weeks. We obtained several clones (named CsR cells), and examined their CsA responses. In contrast to the wild-type MH14#12 replicon cell, which showed an approximately 2-log reduction of HCV-RNA level by treatment with 1 μg/mL CsA for 7 days, all the clones isolated (the results of three representative clones, CsR#4, CsR#10, and CsR#11 cells are shown here) demonstrated resistant phenotypes against CsA with no significant reduction of HCV-RNA by CsA treatment at 1 μg/mL (Fig. 3). The resistance of these clones was thought to arise as a result of (1) mutations on the HCV-RNA genome or (2) alterations in cellular factors. To test the first possibility, we investigated whether HCV-RNA itself in CsR#11 could induce the CsA resistance to naïve cells. Fresh Huh7 cells were transfected with total RNA, including HCV replicon RNA, extracted from CsR#11 cells or MH14#12 cells as controls and cultured for 3 weeks in the presence of G418 (Fig. 1). The resulting colonies were isolated and propagated individually (named cell clones from total RNA of wild-type MH14#12, MH14#12-1, MH14#12-4, and MH14#12-5 cells, and those from CsR#11, CsR#11-2, CsR#11-3, and CsR#11-5 cells). The HCV-RNA titer in MH14#12-derived cells was reduced approximately to 100th by treatment with 1 μg/mL CsA for 7 days (Fig. 4). In contrast, cell clones generated from CsR#11 cells retained a normal HCV titer level after treatment with CsA, indicating that they had lost their sensitivity to CsA. Thus, it was suggested that the CsA-resistant profile in CsR#11 cells was attributed to its HCV-RNA.

D320E mutation in NS5A confers HCV replicon resistance to CsA. In order to identify the mutation in the HCV genome that resulted in the resistance to CsA, HCV subgenomic RNA isolated from CsR#11 cells was sequenced across the subgenomic region encoding non-structural proteins. We found three specific base changes that resulted in amino acid alteration including changes from glutamine to arginine, and isoleucine to threonine at positions 86 (Q86R) and 252 (I252T) in NS3, respectively, and a change from aspartic acid to glutamic acid at position 320 (D320E) in NS5A. Given that all these three mutations, Q86R, I252T, and D320E, were retained in every replicon in CsR#11-2, CsR#11-3, and CsR#11-5 cells, it is likely that they are inherited from CsR#11 cells and are associated with the acquired CsA-resistant phenotype. To examine this possibility, we synthesized replicon RNA carrying all these three mutations and established cells carrying these replicons. The resultant cell clones were named Q86R/I252T/D320E-1 and -3 cells. Treatment of these cells with 1 μg/mL CsA decreased the HCV titer only

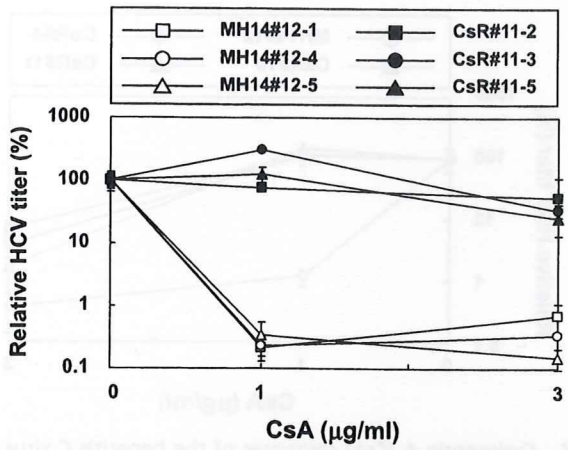

Fig. 4. Hepatitis C virus (HCV) RNA alteration contributed to cyclosporin A (CsA)-resistance. Total RNA extracted from CsA-resistant CsR#11 cells or that from wild-type MH14#12 cells as a control was transfected into Huh7 cells. Colonies established after 4-week selection with G418 were isolated, propagated individually, and tested for CsA response. Three cell clones derived from MH14#12 cells, MH14#12-1, MH14#12-4, and MH14#12-5 cells, and three cell clones from CsR#11 cells, CsR#11-2, CsR#11-3, and CsR#11-5 cells, were treated with 1 and 3 μg/mL CsA for 7 days. HCV-RNA titers were quantified by real-time RT-PCR analysis. The dots represent the means of three independent experiments.

by 1 log, in contrast to the wild-type MH14 clone, in which CsA decreased HCV-RNA by more than 2 logs under the same experimental condition (Fig. 5b). Thus, these mutations were demonstrated to confer CsA resistance; in addition to this, some cellular factors in Huh7 cells may also play minor roles in modulating the CsA sensitivities, given the result that Q86R/I252T/D320E cell clones were relatively sensitive to CsA compared with CsR#11-derived cell clones as shown in Figure 4. We next aimed to determine which of the three mutations, Q86R/I252T/D320E, was responsible for the CsA resistant phenotype, and individual mutations were engineered back into the wild-type MH14 replicon and stable replicon cells were produced as described above. Among three single amino acid mutations, the I252T mutation in NS3 resulted in a significant reduction in replication fitness (Fig. 5a), and almost failed to produce cell colonies. Cell clones harboring MH14 with both Q86R and D320E mutations, Q86R/D320E-2 and Q86R/D320E-3 cells, showed reduced sensitivity to CsA that was comparable to the levels in Q86R/I252T/D320E cells, suggesting Q86R and/or D320E mutation(s) was enough to confer the resistance. Subsequently, we treated the replicon cell clones carrying MH14 with either Q86R or D320E mutation alone, Q86R (Q86R-1 and -4 cells) and D320E (D320E-1 and -2 cells) cells, with CsA for 1 week. The titer of Q86R replicons was reduced to less than 100th by CsA treatment at a concentration of 1 μg/mL, similar to the wild type. In contrast, HCV replicon with D320E mutation in NS5A exhibited reduced sensitivity to CsA, resulting in little reduction of HCV-RNA by the treatment with 1 μg/mL CsA (Fig. 5b). Q86R mutation considerably enhanced colony

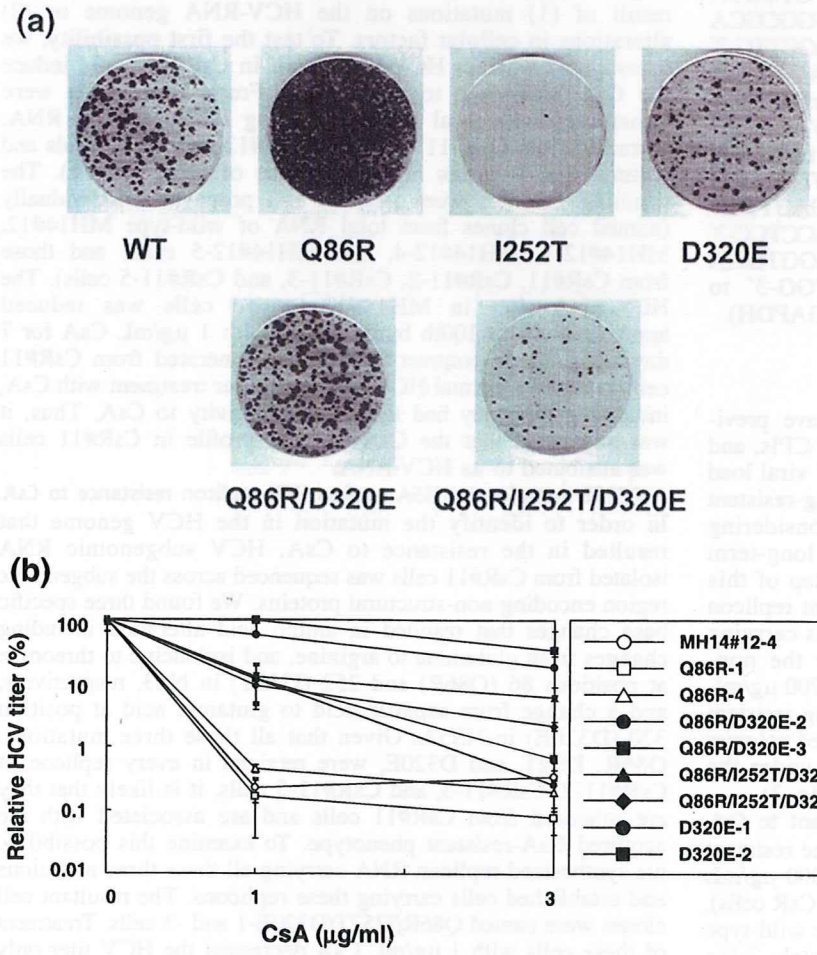

Fig. 5. The amino acid mutation D320E in NS5A conferred the cyclosporin A (CsA)-resistance to hepatitis C virus (HCV) replicons. (a) Colony formation assay for replicons carrying mutations. Five-microgram replicon RNA carrying the mutation(s), Q86R in NS3, I252T in NS3, D320E in NS5A, Q86R and D320E, or Q86R, I252T and D320E, or wild-type RNA transcribed *in vitro* were transduced into Huh7 cells. After culture with G418 for 4 weeks, colonies were stained with crystal violet. (b) Cell clones with replicons carrying indicated mutations were treated with 1 and 3 μg/mL CsA for 7 days. HCV-RNA titers were quantified by real-time RT-PCR analysis. The dots represent the means of three independent experiments. MH14#12-4, wild-type replicon; Q86R-1 and Q86R-4, replicon with Q86R mutation; D320E-1 and D320E-2, replicon with D320E mutation; Q86R/D320E-2 and Q86R/D320E-3, replicon with both Q86R and D320E mutations; Q86R/I252T/D320E-1 and Q86R/I252T/D320E-3, replicon with all three mutations, Q86R, I252T, and D320E.

doi: 10.1111/j.1349-7006.2009.01263.x

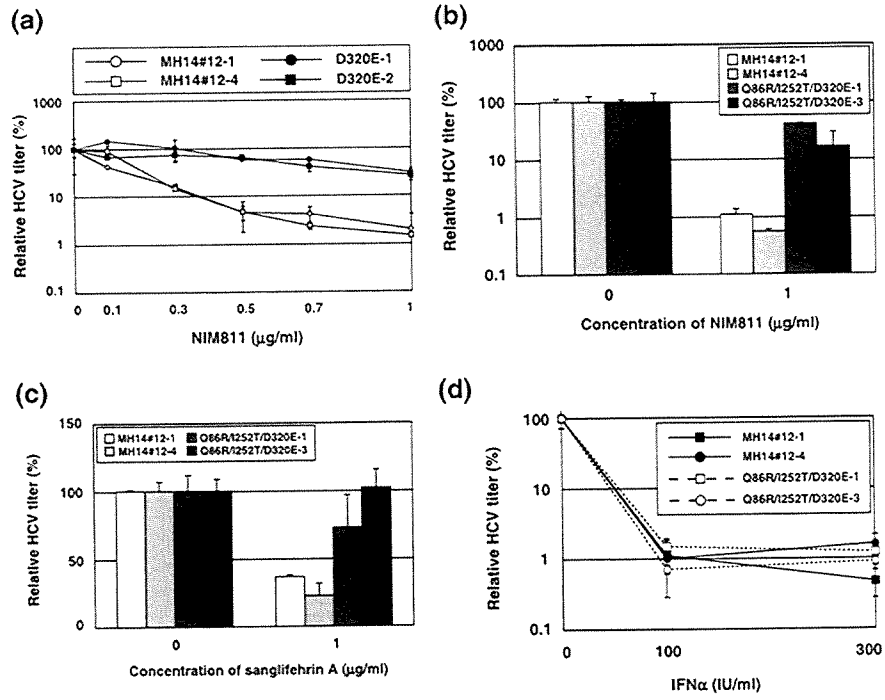

Fig. 6. Cyclosporin A (CsA)-resistant replicons demonstrated cross resistance to additional cyclophilin (CyP) inhibitors, NIM811 and sanglifehrin A (SFA), but not interferon (IFN)-α. MH14#12-1, MH14#12-4, D320E-1 and D320E-2 cells were treated with NIM811 at 0.1, 0.3, 0.5, 0.7 and 1 μg/mL (a), and MH14#12-1, MH14#12-4, Q86R/I252T/D320E-1, and Q86R/I252T/D320E-3 cells were treated with 1 μg/mL NIM811 (b), 1 μg/mL SFA (c), and 100 and 300 IU/mL IFN-α (d) for 7 days. The amounts of hepatitis C virus (HCV) RNA were quantified by real-time RT-PCR analysis. The data represent the means of three independent experiments.

formation efficiency and the D320E mutation showed little significant effect on the efficiency (Fig. 5a). Thus, the D320E mutation in NS5A was suggested as a sufficient factor to induce HCV replicon resistance to CsA, while the Q86R mutation was likely not to contribute to the resistance but to augment the efficiency of HCV replication itself.

The point mutation in NS5A conferred resistance to CPIs. Next, we examined cross-resistance between CsA and other CPIs or IFNα using the CsA-resistant replicon we produced above. Treatment with 0.1–1 μg/mL NIM811 for 7 days showed that the response to NIM811 of D320E-1 and -2 cells was less compared with that of MH14#12-1 and -4 cells, indicating that a CsA-resistant clone also acquired NIM811 resistance (Fig. 6a). A similar result was seen using Q86R/I252T/D320E cells (Fig. 6b). We then tested the anti-HCV activity of SFA, an additional CPI possessing distinct chemical backbone from those of cyclosporins.[16,17] Treatment with 1 μg/mL SFA reduced HCV replication in the wild-type cells, MH14#12-1, and -4 cells; however, it did not significantly reduce replication in Q86R/I252T/D320E cells (Fig. 6c). These results demonstrate that the CsA-resistant cells described in this study were also resistant to additional CPIs, confirming that these two compounds exerted anti-HCV effects via targeting CyP. Finally, we treated Q86R/I252T/D320E cell clones with 100 and 300 IU/mL IFNα for 7 days, and HCV-RNA titers were reduced by 2 logs in both clonal cell lines examined, Q86R/I252T/D320E-1 and Q86R/I252T/D320E-3 cells, as well as in wild-type MH14#12-derived cells, MH14#12-1, and MH14#12-4 cells (Fig. 6d). These results suggested no cross-resistance between CsA and IFNα, consistent with the previous report that the anti-HCV activity of CsA was independent of the IFNα signaling pathway.[18]

The role of CyP subtypes in HCV replication. We have previously reported that CyPB played a significant role in the efficient replication of HCV and CsA inhibited CyPB-mediated regulation of HCV replication. We have also suggested the involvement of other CyP subtypes in HCV replication.[19] To gain further insight into mechanisms underlying the anti-HCV properties of CPIs, we examined the roles of individual CyP subtypes in HCV replication in the wild-type MH14#12-1 and -4 replicon cells. In order to achieve this we knocked down CyPB with siRNAs (Fig. 7d), siCyPB-1 and -2, and found that this procedure reduced the amount of replicons to approximately half the initial level (Fig. 7c), a result consistent with the previous reports. Knockdown of CyPC, CyPE, CyPF, and CyPG (Fig. 7b) did not significantly affect the viral replication under these experimental conditions (Fig. 7a). Some groups have also suggested a role of CyPA in HCV replication.[20,21] Then, we synthesized individual siRNAs reported so far to be effective against CyPA, siCyPA-161, siCyPA-285, and siCyPA-459, and transfected them using a reagent with low cytotoxic activity to knock down endogenous CyPA (Fig. 7d). As shown in Figure 7c, the siRNAs directed against CyPA reduced HCV titers in MH14#12-1, and -4 cells. We previously observed that knockdown of CyPA little affected HCV replication in MH14 cells.[5] Here, by using a new transfection reagent with less cytotoxicity and higher knockdown efficiency, we observed the effect of CyPA knockdown on HCV replication, which suggests that CyPA-mediated regulation of HCV replication is strictly influenced by CyPA's expression level and cellular condition. Under this experimental condition, our RNAi experiments also displayed that knockdown of CyP40 (Fig. 7g), alternatively known as peptidylprolyl isomerase D (NM_005038), decreased the HCV titer (Fig. 7f) without significant cytotoxic effects, presenting CyP40 as additional cellular factor required for HCV replication.

CyPA was related to the CsA-resistant phenotype. We next asked which CyP subtype among CyPA, B, and 40 was related to the CsA resistance observed in our clones. To answer this question, we performed RNAi experiments in the CsA-resistant cell lines, CsR#11-2 and CsR#11-3 cells. Transfection of these cells with specific CyPB or CyP40 siRNAs resulted in the reduction of each subtype (Fig. 7d,g) and decreased the amount of HCV-RNA in CsR#11-derived cells and wild-type MH14#12-derived cells by approximately 50% (Fig. 7c,f). Thus, CyPB and CyP40 were likely to play roles in viral replication, even in the CsA-resistant cells. However, relative HCV titers were not reduced by CyPA knockdown in these CsA-resistant cells in contrast to the case with the wild-type replicon cells (Fig. 7c). A similar resistant phenotype to CyPA knockdown was observed in D320E

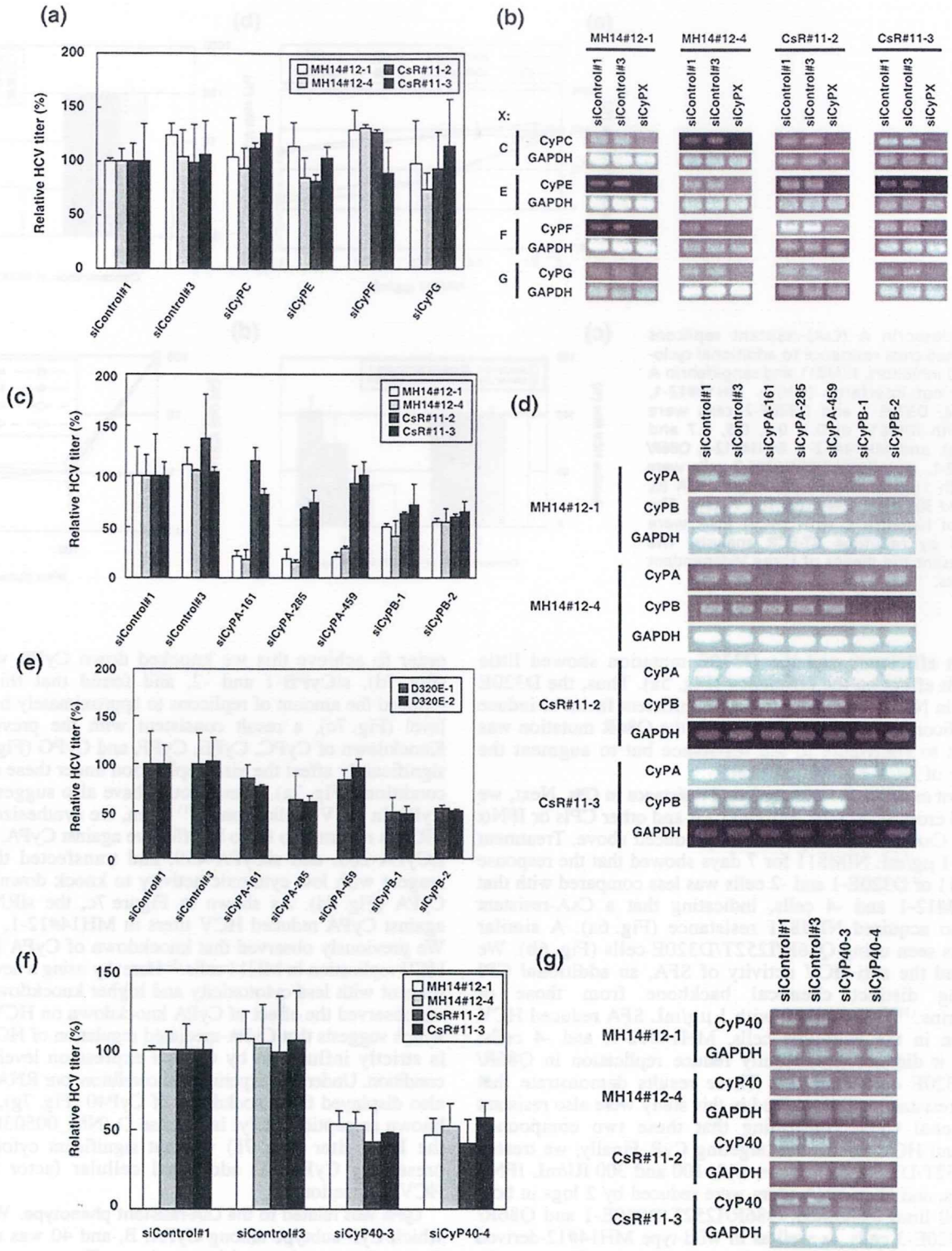

Fig. 7. Cyclophilin (CyP) subtypes related to anti-hepatitis C virus (HCV) effect of CyP inhibitor. MH14#12-derived cells, MH14#12-1 and MH14#12-4 cells, and CsR#11-2 and CsR#11-3 cells, were transfected with siRNAs specific for CyPC (siCyPC), CyPE (siCyPE), CyPF (siCyPF), and CyPG (siCyPG) (a); or those specific for CyPA (siCyPA-161, siCyPA-285, and siCyPA-459) and CyPB (siCyPB-1 and siCyPB-2) (c); or those specific for CyP40 (siCyP40-3 and siCyP40-4) (f); or randomized siRNA controls (siControl#1 and siControl#3). D320E cells were also transfected with the above siRNAs specific for either CyPA or CyPB (e). At 5 days post-transfection, the levels of HCV-RNA were quantified by real-time RT-PCR analysis. The mRNA levels of individual CyP subtypes, CyPC, CyPE, CyPF, and CyPG (CyPX corresponds to each CyP subtype indicated on the left side of the panels) (b), or CyPA and CyPB (d), or CyP40 (g) were measured using glyceraldehydes-3-phosphate dehydrogenase (GAPDH) as internal controls by RT-PCR analysis at 5 days post-transfection. The data represent the means of three independent experiments.

doi: 10.1111/j.1349-7006.2009.01263.x

cell clones (Fig. 7e), showing that CyPA was related to the CsA-resistance conferred by D320E mutation. The CsA-resistant clones obtained in this study were likely to have acquired CyPA independence for efficient HCV replication.

Discussion

Given that CPIs suppressed HCV viral load in cell culture and in patients with chronic hepatitis C,[14,15] CPIs are expected to be new anti-HCV agents. It is important to further reveal the factors related to CPI's anti-HCV activities, thinking over the practical use of CPIs with maximized efficacy and high specificity facing challenges such as side effects and the emergence of resistance to them in clinical settings. Here, we isolated and characterized a variant resistant to CPIs using a HCV subgenomic replicon system. A mutation in NS5A, D320E, was shown to confer the CPI-resistance to HCV replicon, resulting in CyPA independence for efficient viral replication. In addition, assessment of a wide range of CyP subtype knockdown experiments found CyP40 to be a new contributor to HCV replication.

Of the mutations identified, Q86R substitution in NS3 dramatically enhanced the capacity of replication. This mutation was observed as compensatory mutation[22] following the selection of replicons resistant to protease inhibitors SCH503034[23] and SCH6.[24] In addition, this mutation also appeared following the passaging of replicon cells in the absence of drug pressure.[25,26] In actuality, this mutation did not contribute to CsA resistance in the replicon cells (Fig. 5b), and thus was thought to be an adaptive mutation similar to that suggested in previous reports. I252T mutation in NS3, on the other hand, severely reduced the replicative fitness of HCV. The significance of I252T mutation under CsA treatment remains to be studied. The alteration of amino acid residue in NS5A, D320E, resulted in the conversion of HCV replicon to that of the CsA-resistant phenotype. There have been no reports of a link between NS5A and individual CyP subtype in the context of HCV replication, though mutations in NS5A were found to be keys for the acquisition of CsA resistance.[27] We have previously reported that CyPB was important for viral replication, but NS5A did not interact with CyPB in MH14 cells.[5] Indeed, in cells harboring replicons with D320E mutation, CyPB was found to contribute to viral replication but was not related to CsA resistance, as knockdown of CyPB diminished the viral titer to approximately half, similar to the case of the wild type. Therefore, other CyP molecules crucial for viral replication were suggested to be involved in the phenomenon of the CsA resistance. CyPA is another CyP subtype recently published to be critical for HCV replication in connection with viral polymerase.[20,21] Our CsA-resistant replicon cells displayed resistance to CyPA knockdown when compared to wild-type replicon, suggesting that CyPA participated in the replication process and the CsA resistance was due in part to resistance to CyPA inhibition. Therefore, it might be possible that NS5A functions coordinated with CyPA for viral replication and D320E mutation could contribute to enhancement of the relation. But NS5A was unable to bind CyPA *in vitro*.[5] NS5A might be regulated by CyPA associated with other cellular or viral factors during HCV replication. The fact that the D320 falls upon one of the two discontinuous domains needed for the interaction with NS5B to functionally modulate it[28,29] lead us to presume influence of NS5A on the reported NS5B–CyPA interaction.[21] In addition to CyPA and CyPB, which have been published to be cellular factors required for HCV replication, the results suggested that another CyP subtype, CyP40, contributed to viral replication. Acting as a molecular chaperone, it is conceivable that CyP40 directly interacts with viral proteins to boost their functions, similar to CyPA and CyPB. Heat shock protein (Hsp) 90 is a well-known chaperone forming complex with CyP40. Recently, Hsp90 was shown to be harnessed by HCV NS5A via the FK-506 binding protein 8 (FKBP8) bridge. FKBP8 is a homologous immunophilin of CyP40 that is required for viral replication.[30] This result led to the hypothesis that CyP40 serves as a linker between viral proteins and Hsp90. CyP40 is also known to associate with estrogen receptor (ESR) and we have published that ESRα escorted NS5B to replication complex (RC).[31] We also speculate CyP40 connected to ESRα may be important for the recruitment or functional reinforcement of viral and cellular factors for HCV replication in RC. Among these CyP subtypes, CyPA dependency was suggested to be one of the determinants of CsA sensitivity. Interestingly, CyPB and CyP40 play significant role in HCV replication even in CsA-resistant replicon cells. Another CPI, NIM811, is also likely to target CyPA, at least in part, to suppress HCV replication, given the cross-resistance of CsA-resistant replicon to MIN811. However, there is still also the possibility that other CyPs mediate anti-HCV effect of NIM811, which needs to be elucidated in future study.

Understanding the profile of CPI-resistance mutations in the HCV genome and the viral and cellular factors involved will aid in the progression of CPI-centered strategies preparing for the problem of drug resistance. In addition, the cells harboring CPI-resistant replicons established here may prove beneficial for further characterization of resistance mechanisms and for the screening of novel compounds with the potential of clinical application to defeat CPI-resistant variants. Also, CyP40 as a contributor to HCV replication could become another specific antiviral target. The information arising from this study is expected to contribute to the successful use of CPIs against a liver carcinogen, HCV.

Acknowledgments

We thank Novartis (Basel, Switzerland) for providing the CsA derivative, NIM811, and SFA. This work was supported by Grants-in-Aid from the Ministry of Health, Labor and Welfare of Japan. This work was also supported by Grants-in-Aid for Cancer Research from the Ministry of Education, Culture, Sports, Science and Technology of Japan, by Grants-in-Aid for the Research for the Future Program from the Japan Society for the Promotion of Science (JSPS), and by Grants-in-Aid for the Program for Promotion of Fundamental Studies in Health Science from the Organization for Pharmaceutical Safety of Japan. K.W. is a recipient of a JSPS Postdoctoral Fellowship for Research Abroad, and K.G. is a recipient of a JSPS Research Fellowship for Young Scientists.

References

1 Sarbah SA, Younossi ZM. Hepatitis C: an update on the silent epidemic. *J Clin Gastroenterol* 2000; **30**: 125–43.
2 Manns MP, McHutchison JG, Gordon SC *et al.* Peginterferon alfa-2b plus ribavirin compared with interferon alfa-2b plus ribavirin for initial treatment of chronic hepatitis C: a randomised trial. *Lancet* 2001; **358**: 958–65.
3 Fried MW, Shiffman ML, Reddy KR *et al.* Peginterferon alfa-2a plus ribavirin for chronic hepatitis C virus infection. *N Engl J Med* 2002; **347**: 975–82.
4 Watashi K, Hijikata M, Hosaka M, Yamaji M, Shimotohno K. Cyclosporin A suppresses replication of hepatitis C virus genome in cultured hepatocytes. *Hepatology* 2003; **38**: 1282–8.
5 Watashi K, Ishii N, Hijikata M *et al.* Cyclophilin B is a functional regulator of hepatitis C virus RNA polymerase. *Mol Cell* 2005; **19**: 111–22.
6 Manns MP, Foster GR, Rockstroh JK, Zeuzem S, Zoulim F, Houghton M. The way forward in HCV treatment – finding the right path. *Nat Rev Drug Discov* 2007; **6**: 991–1000.
7 McGovern BH, Abu Dayyeh BK, Chung RT. Avoiding therapeutic pitfalls: the rational use of specifically targeted agents against hepatitis C infection. *Hepatology* 2008; **48**: 1700–12.
8 Melnikova I. Hepatitis C therapies. *Nat Rev Drug Discov* 2008; **7**: 799–800.

9 Cordes F, Kaiser R, Selbig J. Bioinformatics approach to predicting HIV drug resistance. *Expert Rev Mol Diagn* 2006; **6**: 207–15.
10 Mo H, Lu L, Dekhtyar T *et al.* Characterization of resistant HIV variants generated by *in vitro* passage with lopinavir/ritonavir. *Antiviral Res* 2003; **59**: 173–80.
11 Molla A, Korneyeva M, Gao Q *et al.* Ordered accumulation of mutations in HIV protease confers resistance to ritonavir. *Nat Med* 1996; **2**: 760–6.
12 Shulman N, Winters M. A review of HIV-1 resistance to the nucleoside and nucleotide inhibitors. *Curr Drug Targets Infect Disord* 2003; **3**: 273–81.
13 Watashi K, Hijikata M, Tagawa A, Doi T, Marusawa H, Shimotohno K. Modulation of retinoid signaling by a cytoplasmic viral protein via sequestration of Sp110b, a potent transcriptional corepressor of retinoic acid receptor, from the nucleus. *Mol Cell Biol* 2003; **23**: 7498–509.
14 Flisiak R, Dumont JM, Crabbe R. Cyclophilin inhibitors in hepatitis C viral infection. *Expert Opin Invest Drugs* 2007; **16**: 1345–54.
15 Flisiak R, Horban A, Gallay P *et al.* The cyclophilin inhibitor Debio-025 shows potent anti-hepatitis C effect in patients coinfected with hepatitis C and human immunodeficiency virus. *Hepatology* 2008; **47**: 817–26.
16 Zhang LH, Liu JO. Sanglifehrin A, a novel cyclophilin-binding immunosuppressant, inhibits IL-2-dependent T cell proliferation at the G1 phase of the cell cycle. *J Immunol* 2001; **166**: 5611–8.
17 Zenke G, Strittmatter U, Fuchs S *et al.* Sanglifehrin A, a novel cyclophilin-binding compound showing immunosuppressive activity with a new mechanism of action. *J Immunol* 2001; **166**: 7165–71.
18 Goto K, Watashi K, Murata T, Hishiki T, Hijikata M, Shimotohno K. Evaluation of the anti-hepatitis C virus effects of cyclophilin inhibitors, cyclosporin A, and NIM811. *Biochem Biophys Res Commun* 2006; **343**: 879–84.
19 Ishii N, Watashi K, Hishiki T *et al.* Diverse effects of cyclosporine on hepatitis C virus strain replication. *J Virol* 2006; **80**: 4510–20.
20 Nakagawa M, Sakamoto N, Tanabe Y *et al.* Suppression of hepatitis C virus replication by cyclosporin A is mediated by blockade of cyclophilins. *Gastroenterology* 2005; **129**: 1031–41.
21 Yang F, Robotham JM, Nelson HB, Irsigler A, Kenworthy R, Tang H. Cyclophilin a is an essential cofactor for hepatitis C virus infection and the principal mediator of cyclosporine resistance *in vitro*. *J Virol* 2008; **82**: 5269–78.
22 Xavier LL, Moya A, Gonzalez-Candelas F. Mapping natural polymorphisms of hepatitis C virus NS3/4A protease and antiviral resistance to inhibitors in worldwide isolates. *Antivir Ther* 2008; **13**: 481–94.
23 Tong X, Chase R, Skelton A, Chen T, Wright-Minogue J, Malcolm BA. Identification and analysis of fitness of resistance mutations against the HCV protease inhibitor SCH 503034. *Antiviral Res* 2006; **70**: 28–38.
24 Yi M, Tong X, Skelton A *et al.* Mutations conferring resistance to SCH6, a novel hepatitis C virus NS3/4A protease inhibitor. Reduced RNA replication fitness and partial rescue by second-site mutations. *J Biol Chem* 2006; **281**: 8205–15.
25 Blight KJ, Kolykhalov AA, Rice CM. Efficient initiation of HCV RNA replication in cell culture. *Science* 2000; **290**: 1972–4.
26 Krieger N, Lohmann V, Bartenschlager R. Enhancement of hepatitis C virus RNA replication by cell culture-adaptive mutations. *J Virol* 2001; **75**: 4614–24.
27 Fernandes F, Poole DS, Hoover S *et al.* Sensitivity of hepatitis C virus to cyclosporine A depends on nonstructural proteins NS5A and NS5B. *Hepatology* 2007; **46**: 1026–33.
28 Shirota Y, Luo H, Qin W *et al.* Hepatitis C virus (HCV) NS5A binds RNA-dependent RNA polymerase (RdRP) NS5B and modulates RNA-dependent RNA polymerase activity. *J Biol Chem* 2002; **277**: 11149–55.
29 Shimakami T, Hijikata M, Luo H *et al.* Effect of interaction between hepatitis C virus NS5A and NS5B on hepatitis C virus RNA replication with the hepatitis C virus replicon. *J Virol* 2004; **78**: 2738–48.
30 Okamoto T, Nishimura Y, Ichimura T *et al.* Hepatitis C virus RNA replication is regulated by FKBP8 and Hsp90. *Embo J* 2006; **25**: 5015–25.
31 Watashi K, Inoue D, Hijikata M, Goto K, Aly HH, Shimotohno K. Anti-hepatitis C virus activity of tamoxifen reveals the functional association of estrogen receptor with viral RNA polymerase NS5B. *J Biol Chem* 2007; **282**: 32765–72.

doi: 10.1111/j.1349-7006.2009.01263.x

The Journal of Immunology

Sustained Exogenous Expression of Therapeutic Levels of IFN-{gamma} Ameliorates Atopic Dermatitis in NC/Nga Mice via Th1 Polarization

Kayoko Hattori, Makiya Nishikawa, Kanitta Watcharanurak, Akihiko Ikoma, Kenji Kabashima, Hiroyasu Toyota, Yuki Takahashi, Rei Takahashi, Yoshihiko Watanabe and Yoshinobu Takakura

J. Immunol. published online Jan 27, 2010;
doi:10.4049/jimmunol.0900215

The Journal of Immunology is published twice each month by The American Association of Immunologists, Inc., 9650 Rockville Pike, Bethesda, MD 20814-3994.

Print ISSN: 0022-1767 Online ISSN: 1550-6606.

Published January 27, 2010, doi:10.4049/jimmunol.0900215

Sustained Exogenous Expression of Therapeutic Levels of IFN-γ Ameliorates Atopic Dermatitis in NC/Nga Mice via Th1 Polarization

Kayoko Hattori,* Makiya Nishikawa,* Kanitta Watcharanurak,* Akihiko Ikoma,† Kenji Kabashima,† Hiroyasu Toyota,* Yuki Takahashi,* Rei Takahashi,‡ Yoshihiko Watanabe,§ and Yoshinobu Takakura*

The short in vivo half-life of IFN-γ can prevent the cytokine from inducing immunological changes that are favorable for the treatment of Th2-dominant diseases, such as atopic dermatitis. To examine whether a sustained supply of IFN-γ is effective in regulating the balance of Th lymphocyte subpopulations, plasmid vector encoding mouse IFN-γ, pCpG-Muγ, or pCMV-Muγ was injected into the tail vein of NC/Nga mice, a model for human atopic dermatitis. A single hydrodynamic injection of a CpG motif reduced pCpG-Muγ at a dose of 0.14 μg/mouse resulted in a sustained concentration of IFN-γ in the serum, and the concentration was maintained at >300 pg/ml over 80 d. The pCpG-Muγ–mediated IFN-γ gene transfer was associated with an increase in the serum concentration of IL-12, reduced production of IgE, and inhibition of mRNA expression of IL-4, -5, -10, -13, and -17 and thymus and activation-regulated chemokine in the spleen. These immunological changes were not clearly observed in mice receiving two injections of 20 μg pCMV-Muγ, a CpG-replete plasmid DNA, because of the transient nature of the expression from the vector. The mice receiving pCpG-Muγ showed a significant reduction in the severity of skin lesions and in the intensity of their scratching behavior. Furthermore, high transepidermal water loss, epidermal thickening, and infiltration of lymphocytes and eosinophils, all of which were obvious in the untreated mice, were significantly inhibited. These results indicate that an extraordinary sustained IFN-γ expression induces favorable immunological changes, leading to a Th1-dominant state in the atopic dermatitis model. ***The Journal of Immunology*****, 2010, 184: 000–000.**

The number of patients with allergies, including those with asthma, pollinosis, and atopic dermatitis, has been increasing in recent decades, especially in developed countries. It is believed that these disorders result from the imbalance of Th lymphocyte subpopulations (Th1 and Th2), which play major roles in the immune response (1). Under normal conditions, the differentiation of naive T cells to Th1 and Th2 lineages is regulated by cytokines that are secreted from various cells, including themselves, and the Th1/Th2 balance is maintained. However, in atopic dermatitis, which is one of the most common type 1 allergic diseases, the balance shifts to Th2 dominance; this eventually leads to excessive Th2 cytokine production. Th2-like immune responses play an important role in the pathogenic mechanism of atopic disorders, because Th2 cytokines mediate excessive IgE production, a major cause of atopic inflammation (2–5).

IFN-γ, a Th1 cytokine, inhibits the differentiation of naive T cells to Th2 cells, as well as the production of Th2 cytokines from Th2 cells. Thus, IFN-γ has been considered to be capable of correcting the Th1/Th2 imbalance and is effective in the treatment of diseases in which the balance is impaired, such as atopic dermatitis (6). Despite such positive features, few attempts have been made to use IFN-γ as a pharmaceutical agent for the treatment of atopic dermatitis (7–10). This is mainly due to the fact that IFN-γ, as well as other IFNs, has a short half-life in vivo, and multiple injections are required to maintain its concentration at levels high enough to prevent dermatitis (11).

Several approaches have been developed to extend the duration of the therapeutic effects of biologically active proteins. Extension of the in vivo half-life of proteins can be achieved by using controlled- or sustained-release systems (12–15) or by chemical modification of proteins (16–18). Pepinsky et al. (19) demonstrated that the high clearance of IFN-β-1a was reduced by PEGylation, and its increased systemic exposure resulted in better antiviral effects. PEGylated IFN-α in combination with an antiviral drug, ribavirin, is now a standard treatment for hepatitis C virus-induced chronic hepatitis. The increased half-life of IFNs obtained by PEGylation has greatly increased their therapeutic efficacy. In addition to these challenges, gene delivery is an option to increase the in vivo half-life of therapeutic proteins, including IFNs. In previous studies, we proved that the depletion of CpG motifs in plasmid vectors is an effective approach for extending the duration of transgene expression (20, 21). We also succeeded in developing a murine IFN-γ–expressing plasmid DNA, pCpG-Muγ, which contains no CpG motifs except for those in the cDNA region (22). A single i.v. injection of pCpG-Muγ resulted in a high and sustained IFN-γ concentration in the serum over 1 mo after hydrodynamic injection into healthy ICR mice. However, little is

*Department of Biopharmaceutics and Drug Metabolism and §Department of Molecular Microbiology, Graduate School of Pharmaceutical Sciences; †Department of Dermatology, Graduate School of Medicine, Kyoto University; and ‡Department of Pharmacotherapeutics, Faculty of Pharmaceutical Sciences, Doshisha Women's College of Liberal Arts, Kyotanabe, Kyoto, Japan

Received for publication January 26, 2009. Accepted for publication December 24, 2009.

Address correspondence and reprint requests to Dr. Makiya Nishikawa, Department of Biopharmaceutics and Drug Metabolism, Graduate School of Pharmaceutical Sciences, Kyoto University, Sakyo-ku, Kyoto 606-8501, Japan. E-mail address: makiya@pharm.kyoto-u.ac.jp

Abbreviations used in this paper: SPF, specific pathogen-free; TARC, thymus and activation-regulated chemokine; TEWL, transepidermal water loss; TNCB, 2,4,6-trinitrochlorobenzene.

www.jimmunol.org/cgi/doi/10.4049/jimmunol.0900215

known about how such a sustained transgene expression of IFN-γ influences the Th1/Th2 balance under Th2-dominant conditions.

In this study, we injected pCpG-Muγ, a murine IFN-γ–expressing plasmid DNA, into a human atopic dermatitis model (NC/Nga mice) (23), to achieve a sustained transgene expression of IFN-γ. A conventional CpG replete plasmid vector expressing IFN-γ, pCMV-Muγ (21, 24), was also used for comparison to examine the importance of the duration of transgene expression on the immunological changes induced by IFN-γ gene transfer. The expression profile of IFN-γ was first examined in NC/Nga mice, and the effect of the expression on the level of IL-4, -5, -10, -12, -13, -17, and thymus and activation-regulated chemokine (TARC) was evaluated. Then, skin lesions, the intensity of scratching behavior, transepidermal water loss (TEWL), the thickness of the epidermis, and the infiltration of the skin by inflammatory cells were evaluated. In this study we showed that sustained, but not transient, gene expression of IFN-γ can induce favorable immunological changes in a human atopic dermatitis model, which allows the prevention of the development of atopic dermatitis-like skin lesions.

Materials and Methods

Animals

Five-week-old male C57BL/6 mice and 6-wk-old male NC/Nga mice that were raised under conventional conditions, but had not developed dermatitis, were purchased from Japan SLC (Hamamatsu, Japan) and maintained on a standard food-and-water diet under conventional housing conditions. The protocol for the animal experiments was approved by the Animal Experimentation Committee of the Graduate School of Pharmaceutical Sciences, Kyoto University.

Plasmid DNA

Two types of IFN-γ–expressing plasmid vectors developed in our laboratory were used: pCMV-Muγ, which was constructed by inserting a murine IFN-γ cDNA fragment into the BamHI site of pcDNA3 (Invitrogen, Carlsbad, CA) (24), and pCpG-Muγ, which was constructed by inserting the BglII/NheI IFN-γ cDNA fragment amplified by PCR from the pCMV-Muγ into the BglII/NheI site of pCpG-mcs (Invivogen, San Diego, CA) (22).

In vivo gene transfer of IFN-γ

Naked plasmid DNA dissolved in isotonic saline solution was injected into the tail vein of mice over 5 s on day 0 (25, 26). To adjust the peak level of the IFN-γ concentration after gene transfer, the plasmid dose was fixed at 0.14 and 20 μg/mouse for pCpG-Muγ and pCMV-Muγ, respectively, based on preliminary experiments. pCMV-Muγ was injected twice at an interval of 1 wk (days 0 and 7). The body weight and temperature of mice were measured to assess the adverse effects of IFN-γ gene transfer.

Measurement of concentration of IFN-γ, IgE, and IL-4, -12, and -13

Blood samples were obtained from the tail vein at indicated times after gene transfer, incubated at 4°C for 2 h to allow clotting, and centrifuged to obtain serum. Dorsal skin tissue was homogenized in PBS containing protease inhibitors (protease inhibitor mixture; Sigma-Aldrich, Munich, Germany) and then centrifuged for 30 min at 12,000 × *g*. The concentration of IFN-γ, IgE, and IL-4, -12, and IL-13 in the serum or supernatant of skin homogenate was measured using ELISA kits (Ready-SET-Go! Mouse IFN-γ and IL-13 ELISA, eBioscience, San Diego, CA; OptEIA set Mouse IL-12, IgE and IL-13, BD Biosciences, San Jose, CA).

mRNA quantification

Total RNA was extracted from ~100 mg spleen or skin sample using Sepasol RNA I Super (Nacalai Tesque, Kyoto, Japan). The total RNA was cleaned up using an RNeasy mini kit (Qiagen, Hilden, Germany). Reverse transcription was performed using a SuperScript II (Invitrogen) and oligo (dT) primer, according to the manufacturer's protocol. For a quantitative analysis of mRNA expression, real-time PCR was carried out with total cDNA using a LightCycler instrument (Roche Diagnostics, Basel, Switzerland). The oligonucleotide primers used for amplification are listed in Table I. Amplified products were detected online via intercalation of the fluorescent dye SYBR green (LightCycler-FastStart DNA Master SYBR Green I kit, Roche Diagnostics, Indianapolis, IN). The cycling conditions were as follows: initial enzyme activation at 95°C for 10 min, followed by 55 cycles at 95°C for 10 s, 60°C for 5 s, and 72°C for 20 s. All cycling reactions were performed in the presence of 3.5 mM $MgCl_2$. Gene-specific fluorescence was measured at 72°C. The mRNA expression of genes of interest was normalized using the mRNA level of β-actin.

Scoring skin lesions

Skin lesions were scored at indicated times after gene transfer, according to the criteria of Matsuda et al. (23). The scoring was based on the severity of eczema, erosion/excoriation, scaling, erythema/hemorrhage, inflammation of the face, and inflammation of the ear. The total clinical skin severity score was defined as the sum of each of the six signs (none = 0; mild = 1; moderate = 2; and severe = 3).

Observation of scratching behavior

On days 7, 14, and 35, scratching behavior was monitored using SCLABA Real (Noveltec, Kobe, Japan), an automated system to analyze the scratching behavior of small animals. Each mouse was put into an acrylic cage, and the behavior of the mice was recorded for 30 min. The number of episodes and the duration of scratching behavior were automatically quantified. In a different set of mice, the scratching behavior was recorded on video for 1 h on days 7, 14, 35, and 84. The videotape was played back at a later time, and the number of scratching episodes was counted manually. A series of scratching behaviors, starting with the stretching of the hind paws to the head, face, or back and ending with the set-back of the paws, was counted as one bout of scratching (27).

Measurement of TEWL

TEWL was measured using a VAPO SCAN (AS-VT 100RS, Asahi Biomed, Yokohama, Japan) on the shaved back of mice.

Analysis of skin sections

The dorsal skin of the mice was excised, fixed in 4% paraformaldehyde, and embedded in paraffin. Then, 4 μm-sections were made using a microtome and stained with H&E for histological evaluation or with toluidine blue to detect mast cells. The numbers of lymphocytes, eosinophils, and mast cells on H&E-stained sections (lymphocytes and eosinophils) or toluidine blue-stained sections (mast cells) were manually counted under a microscope and expressed as the number per unit length of skin section.

Effect of IFN-γ gene transfer on 2,4,6-trinitrochlorobenzene-induced dermatitis

To assess whether IFN-γ gene transfer increases the risk for contact dermatitis, C57BL/6 mice were sensitized by painting 25 μl 3% 2,4,6-trinitrochlorobenzene (TNCB) in acetone/olive oil (4:1) on the shaved abdomen (day 0). pCpG-Muγ was injected by the hydrodynamic injection method to TNCB-treated mice 1 d before or 7 d after the TNCB treatment, at a dose of 0.14 μg/mouse. On day 5, the thickness of the ear was measured with a Quick Mini thickness gauge (Mitutoyo, Tokyo, Japan). Then, 20 μl 1.5% TNCB solution was applied to the surface of the ear. The thickness of the ear was measured again 24 h after the second application (challenge), and ear swelling was evaluated by the difference in the thickness before and after the challenge.

Effect of IFN-γ gene transfer on TEWL in tape stripping- and TNCB-induced dermatitis models

C57BL/6 mice were shaved on their dorsal skin on day 0 and injected with pCpG-Muγ (0.14 μg/mouse) or saline by the hydrodynamic injection method on the same day. Mice were repeatedly treated with 50 μl 1% TNCB dissolved in acetone/olive oil (4:1) to the shaved skin on days 1, 8, 11, and 13. In a separate experiment, the dorsal skin of C57BL/6 mice was tape stripped on days 1 and 8 and injected with pCpG-Muγ (0.14 μg/mouse) or saline by the hydrodynamic injection method on day 0. TEWL from the stripped or shaved skin was measured as described above.

Statistical analysis

Differences were evaluated by the Student *t* test, and the level of statistical significance was $p < 0.05$.

Results

IFN-γ concentration in the serum of NC/Nga mice after injection of IFN-γ–expressing plasmid DNA

Fig. 1 shows the time courses of the concentration of IFN-γ in the serum after i.v. injection of pCpG-Muγ or pCMV-Muγ. A very high and sustained concentration of IFN-γ was detected in the

serum of mice receiving pCpG-Muγ at a dose of 0.14 μg/mouse: >300 pg IFN-γ/ml was detected ~3 mo after a single injection. However, the concentration of IFN-γ had decreased very quickly below the detection limit (25 pg/ml) 3 d after the first injection of pCMV-Muγ (20 μg/mouse). The plasmid was injected again 1 wk later, but the peak level was lower than that after the first injection, and the concentration decreased quickly again.

IL-12 concentration in the serum of NC/Nga mice after injection of IFN-γ–expressing plasmid DNA

It would be expected that a persistent expression of IFN-γ would induce the expression of IL-12, a typical Th1 cytokine that promotes the differentiation of naive T cells into the Th1 phenotype. Therefore, the serum concentration of IL-12 was measured (Fig. 2*A*). The IL-12 concentration in the untreated group was not constant during the experimental period; it fluctuated, reflecting the acute and chronic phases of the disease (28). The concentration of IL-12 was significantly increased in the pCpG-Muγ–treated group from days 3 to 42 after injection. The concentration in the pCMV-Muγ–treated group was significantly greater 3 d after the first injection compared with that in the untreated group; thereafter, the profile became superimposed on that of the untreated group. The second injection of pCMV-Muγ on day 7 barely affected the serum concentration of IL-12.

IgE concentration in the serum of NC/Nga mice after injection of IFN-γ–expressing plasmid DNA

Next, the concentration of IgE, a diagnostic marker of atopic dermatitis (29), was measured in the serum, because increased IgE production is a hallmark of Th2 immune responses. Fig. 2*B* shows the concentration of IgE in the serum of the untreated mice or mice treated with pCpG-Muγ or pCMV-Muγ. The concentration at the onset of treatment was ~10 μg/ml, and it increased with time to >100 μg/ml in the untreated group. It also increased in the treated groups, but the increase was significantly inhibited in the pCpG-Muγ–treated group at ≥14 d after the treatment. In addition, we measured the serum concentrations of IL-4 and -13, which play important roles in the regulation of IgE synthesis (30). However, the concentrations of IL-4 and -13 in the serum of all groups were below the detection limit (4 pg/ml) of the analysis.

mRNA expression of cytokine and chemokine in spleen cells of NC/Nga mice after injection of IFN-γ–expressing plasmid DNA

The effect of IFN-γ gene transfer on the expression of cytokines/chemokines was evaluated by measuring the mRNA expression of IL-12, Th2 cytokines (IL-4, -5, -10, and -13), IL-17, and a Th2 chemokine (TARC) in spleen cells collected from mice 14 d after gene transfer using the primers listed in Table I. The mRNA expression of these genes in spleen cells was normalized to that of β-actin, and the ratios were compared between the untreated and the pCpG-Muγ–treated mice (Fig. 3). The differences between the groups were very large for IL-5, -10, -12, and -13 and TARC, although they were not statistically significant because of the limited number of samples. The IL-12 mRNA expression was increased by injection of pCpG-Muγ, which was in good agreement with the serum level of IL-12 (Fig. 2*A*). The mRNA expression of IL-4, -5, -10, -13, and -17 and TARC in the pCpG-Muγ–treated group was lower than that in the untreated group. The mRNA expression in spleen cells 40 d after gene transfer showed no significant differences (data not shown). In addition, the expression of these cytokines in the skin was examined by ELISA and RT-PCR 40 d after gene transfer. However, no significant differences were detected among the groups (data not shown).

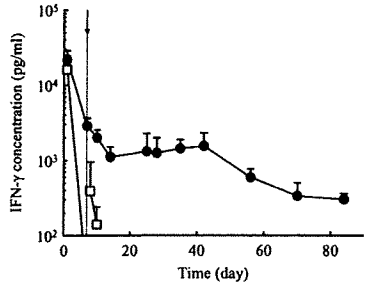

FIGURE 1. Time course of the concentration of IFN-γ in mouse serum after injection of IFN-γ–expressing plasmid DNA. NC/Nga mice were injected i.v. with 0.14 μg pCpG-Muγ (●) or 20 μg pCMV-Muγ (□) by the hydrodynamic injection method. The pCMV-Muγ–injected group received a second injection of 20 μg pCMV-Muγ 7 d after the first injection (indicated by a dashed line and an arrow). The results are expressed as the mean ± SD of five mice.

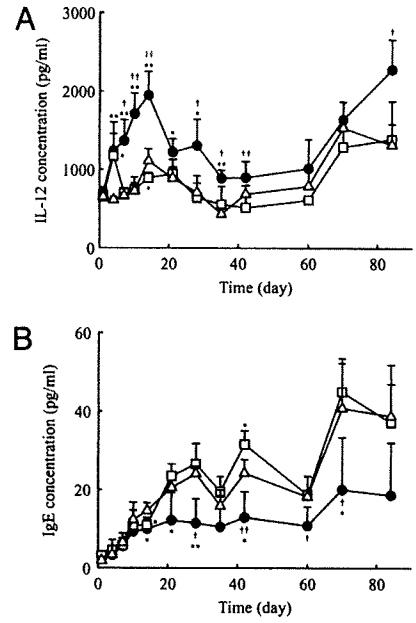

FIGURE 2. Time course of the concentration of IL-12 (*A*) and IgE (*B*) in mouse serum after injection of IFN-γ–expressing plasmid DNA. NC/Nga mice were injected i.v. with 0.14 μg pCpG-Muγ or 20 μg pCMV-Muγ, as described in the legend of Fig. 1. Blood samples from untreated (△), pCpG-Muγ–injected (●), or pCMV-Muγ–injected (□) mice were collected from the tail vein at the indicated times after gene transfer. The results are expressed as the mean ± SD of at least three mice. $*p < 0.05$ compared with the untreated group; $**p < 0.01$ compared with the untreated group; $^{\dagger}p < 0.05$ compared with the pCMV-Muγ–treated group; $^{\dagger\dagger}p < 0.01$ compared with the pCMV-Muγ–treated group.

Table I. *Primer sequences for quantitative RT-PCR*

Gene	Forward Primer (5′→3′)	Reverse Primer (5′→3′)
Mouse β-actin	gcaccacaccttctacaatgag	ttggcatagaggtctttacgga
Mouse IL-12	catcgatgagctgatgcagt	cagatagcccatcaccctgt
Mouse IL-4	gcttttcgatgcctggattc	gctttccaggaagtctttcagtg
Mouse IL-5	agagaagtgtggcgaggagaga	cattgcccactctgtactcatca
Mouse IL-10	ttgccaagccttatcgga	ttctgggccatgcttctct
Mouse IL-13	cagctccctggttctctcac	ccacactccataccatgctg
Mouse IL-17	tccagaaggccctcagacta	agcatcttctcgaccctgaa
Mouse TARC	agtggagtgttccagggatg	gtcacaggccgctttatgtt

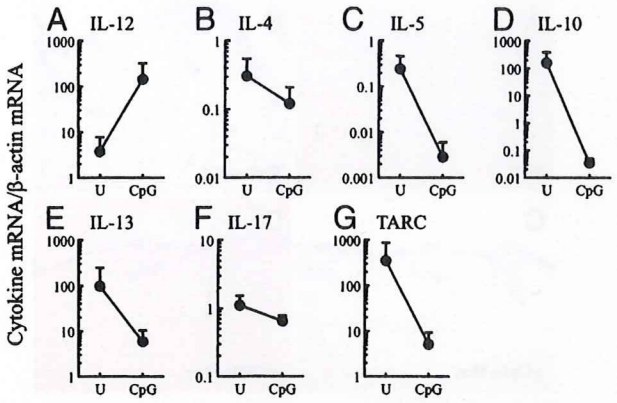

FIGURE 3. mRNA expression of cytokines and TARC in spleen cells. Spleens from NC/Nga mice receiving 0.14 μg pCpG-Muγ (CpG) were collected 14 d after gene transfer, and the mRNA expression of cytokine and chemokine genes was measured by real-time PCR. The mRNA expression of genes was normalized using the mRNA level of β-actin. In comparison, spleens from untreated mice (U) were treated as above. *A*, IL-12. *B*, IL-4. *C*, IL-5. *D*, IL-10. *E*, IL-13. *F*, IL-17. *G*, TARC. The results are expressed as the mean ± SD of three mice.

Skin lesions of NC/Nga mice after injection of IFN-γ–expressing plasmid DNA

The results indicated that the Th1/Th2 balance can be shifted to Th1 in the atopic dermatitis model by sustained, but not transient, transgene expression of IFN-γ. The effects of gene transfer on atopic dermatitis were examined in NC/Nga mice. Fig. 4 shows the typical images of the back skin of mice 35 d after the start of treatment. Clinical signs and symptoms were clearly seen on the skin of the untreated mice (Fig. 4*A*) and the pCMV-Muγ–treated mice (Fig. 4*C*), indicating that these mice developed a severe dermatitis. The severity of skin damage was scored using a clinical skin score (23). The untreated and the pCMV-Muγ–treated groups developed dermatitis within a week after the start of the experiment, and the severity of the dermatitis increased with time (Fig. 4*D*). In contrast, the pCpG-Muγ–treated mice developed much less severe skin inflammation throughout the experimental period (Fig. 4*B*), and the clinical skin score of the group was significantly lower than that of the untreated or the pCMV-Muγ–treated group (Fig. 4*D*).

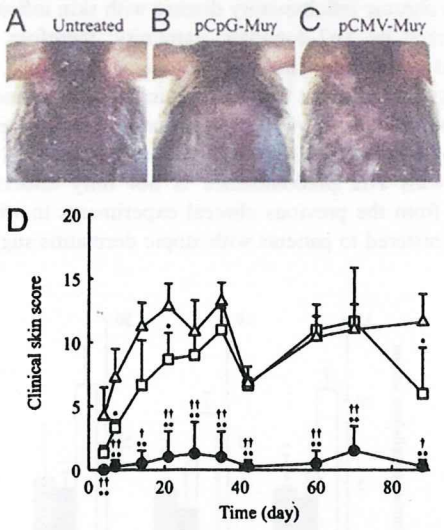

FIGURE 4. Typical images of the back skin of NC/Nga mice (*A–C*) and the time course of the skin clinical score (*D*). Photographs were taken 35 d after the start of treatment. *A*, Untreated mice. *B*, pCpG-μγ–treated mice. *C*, pCMV-μγ–treated mice. *D*, Clinical features of dermatitis were scored at indicated periods of time after the start of treatment. The results are expressed as the mean ± SD of at least three mice. $*p < 0.05$ compared with the untreated group; $**p < 0.01$ compared with the untreated group; $^{\dagger}p < 0.05$ compared with the pCMV-Muγ–treated group; $^{\dagger\dagger}p < 0.01$ compared with the pCMV-Muγ–treated group.

Scratching behavior of NC/Nga mice after injection of IFN-γ–expressing plasmid DNA

Fig. 5 shows the number of episodes of scratching and the cumulative time of scratching for a 30-min period. The number and duration of scratching episodes increased with time in the untreated group. The pCpG-Muγ– and pCMV-Muγ–treated groups had significantly fewer episodes and shorter duration of scratching than the untreated group, with significantly better results for pCpG-Muγ–treated mice. Similar results were obtained in a different set of mice whose scratching episodes were counted manually after videotaping (data not shown).

TEWL of NC/Nga mice after injection of IFN-γ–expressing plasmid DNA

Dry skin is a common symptom of atopic dermatitis, which is characterized by extensive water loss through the skin. Thus, the TEWL of the skin was measured on the back (Fig. 6). The TEWL value at day 0 was ~10 g/h/m^2 in all groups. In the untreated mice, the value increased to >50 g/h/m^2 by day 14, and an almost constant value was observed in the period that followed. The elevation of TEWL was significantly inhibited in the pCpG-Muγ–treated group throughout the experimental period. The TEWL of the pCMV-Muγ–treated mice was as low as that of the pCpG-Muγ–treated ones for the first 14 d, but it was significantly higher at days 70 and 84.

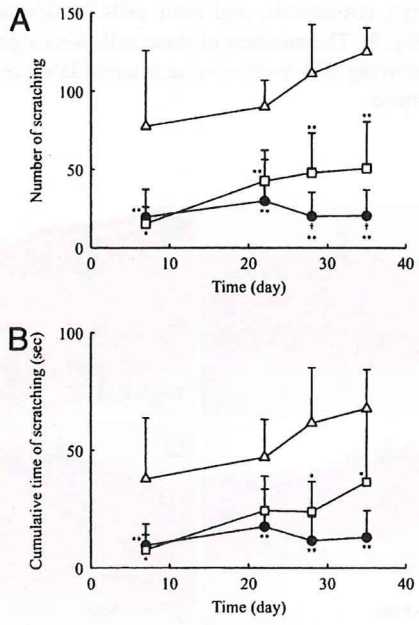

FIGURE 5. Number (*A*) and cumulative time (*B*) of scratching episodes. Scratching behavior of NC/Nga mice treated as described in the legend of Fig. 1 were automatically evaluated using SCLABA-Real. △, untreated mice; ●, pCpG-Muγ–treated mice; □, pCMV-Muγ–treated mice. The results are expressed as the mean ± SD of at least three mice. $*p < 0.05$ compared with the untreated group; $**p < 0.01$ compared with the untreated group; $^{\dagger}p < 0.05$ compared with the pCMV-Muγ–treated group.

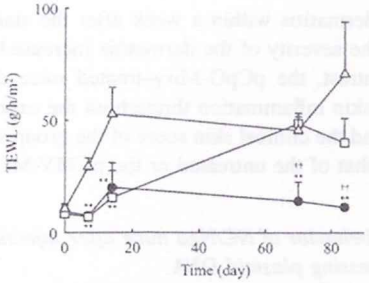

FIGURE 6. Time course of the TEWL of the back skin of mice. TEWL was measured on the back of untreated mice (△), pCpG-Mug–treated mice (●), and pCMV-Mug–treated mice (□). The results are expressed as the mean ± SD of at least three mice. $^{**}p < 0.01$ compared with the untreated group; $^{\dagger\dagger}p < 0.01$ compared with the pCMV-Muγ–treated group.

Histological examination of skin sections of NC/Nga mice after injection of IFN-γ–expressing plasmid DNA

Fig. 7 shows the H&E sections of the back skin of treated and untreated mice at day 14 after the start of treatment. NC/Nga mice maintained under specific pathogen-free (SPF) conditions were used as control mice with healthy skin; the skin sections from the SPF control mice showed no pathological features (Fig. 7*A*). In marked contrast, there was clear hyperplasia of the epidermis (acanthosis) in the untreated group (Fig. 7*B*). The sections from the untreated mice also showed an extensive infiltration of lymphocytes and eosinophils. These characteristic features of inflamed skin tissues were not as apparent in the skin sections from the pCpG-Muγ–treated mice (Fig. 7*C*), which were indistinguishable from the skin sections from the SPF control mice. Compared with the sections from the pCpG-Muγ–treated mice, the ones from pCMV-Muγ–treated mice showed less significant improvement (Fig. 7*D*). Fig. 8 shows the skin sections in which mast cells were stained with toluidine blue. Again, a significant infiltration of mast cells was observed in the untreated mice (Fig. 8*B*), but not in the SPF control (Fig. 8*A*) or the pCpG-Muγ–treated mice (Fig. 8*C*). The numbers of lymphocytes, eosinophils, and mast cells in skin sections were counted (Fig. 9). The numbers of these cells were significantly less in mice receiving IFN-γ–expressing plasmid DNA compared with untreated mice.

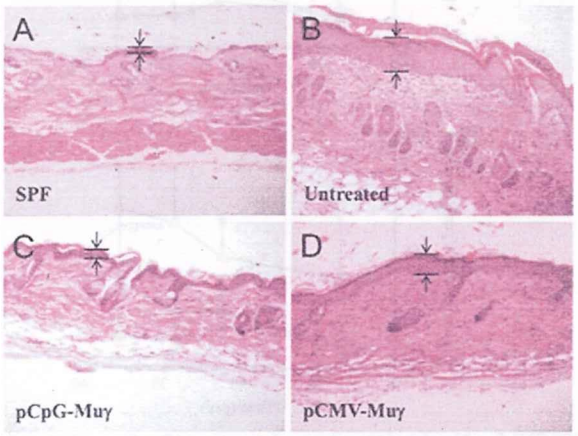

FIGURE 7. H&E sections of the back skin of NC/Nga. Dorsal skin of mice maintained under SPF conditions (*A*), untreated mice (*B*), pCpG-μγ–treated mice (*C*), and pCMV-μγ–treated mice (*D*) were collected at day 14. Skin sections were stained with H&E for histological evaluation and detection of inflammatory cells. Arrows and bars indicate the thickness of the epidermis. Original magnification ×400.

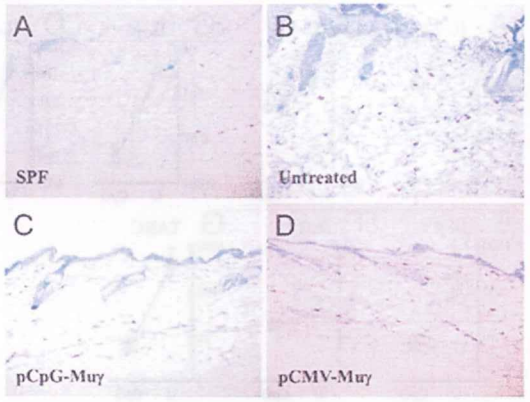

FIGURE 8. Toluidine blue sections of the back skin of NC/Nga mice. Dorsal skin of mice maintained under SPF conditions (*A*), untreated mice (*B*), pCpG-Muγ–treated mice (*C*), and pCMV-Muγ–treated mice (*D*) were collected at day 14. Skin sections were stained with toluidine blue to detect mast cells. Original magnification ×400.

Adverse effects of IFN-γ gene transfer

There were no significant differences in the body weight or temperature between the saline-injected mice and the pCpG-Muγ–treated mice. To examine whether IFN-γ gene transfer increases the risk for contact dermatitis, the ear thickness was measured in a mouse model of TNCB-induced contact dermatitis. The challenge with TNCB significantly increased the thickness, but the injection of pCpG-Muγ had no significant effects on the change (data not shown). Fig. 10 shows the time courses of the TEWL from the dorsal skin of tape stripped (Fig. 10*A*) or TNCB-treated mice (Fig. 10*B*). Again, no IFN-γ gene transfer-induced increase was observed in any case examined.

Discussion

Because of the multiple functions of cytokines and their complicated network, the effects of externally administered cytokines, including IFN-γ, depend on their pharmacokinetics. Atopic dermatitis, a chronic inflammatory disease with skin inflammation, is characterized by Th2-dominant immunity; therefore, any treatment that normalizes the Th1/Th2 balance can be useful for treatment of the disease. IFN-γ, a typical Th1 cytokine, has been considered to induce a variety of immunological changes, leading to a Th1-dominant state, but its effects on the Th1/Th2 balance in patients with Th2 predominance is not fully understood. The outcome from the previous clinical experiments in which IFN-γ was administered to patients with atopic dermatitis suggested that

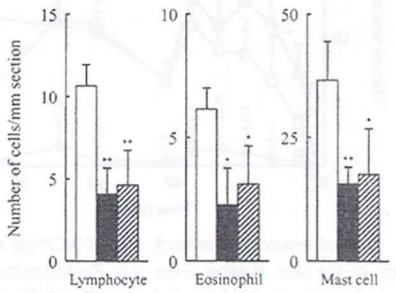

FIGURE 9. Number of lymphocytes, eosinophils, and mast cells in skin sections. Lymphocytes and eosinophils in H&E-stained sections were counted under a microscope. The toluidine blue sections were used for the counting of mast cells. The number of cells was expressed as the mean ± SD of three sections: untreated mice (open bars), pCpG-Muγ–treated mice (filled bars), and pCMV-Muγ–treated mice (striped bars).